

Disentangling Sex-Dependent Effects of APOE on Diverse Trajectories of Cognitive Decline in Alzheimer's Disease

Running title: Elucidating Multi-Stage Progression of Neuroimaging Biomarkers in Alzheimer's Disease

Haixu Ma¹, Zhuoyu Shi², Minjeong Kim³, Bin Liu⁴ Patrick J. Smith², Yufeng Liu^{1,6+}, Guorong Wu^{1,2,5,7,*}, and Alzheimer's Disease Neuroimaging Initiative (ADNI)

¹ Department of Statistics and Operations Research, University of North Carolina at Chapel Hill, NC 27955, USA

² Department of Psychiatry, University of North Carolina at Chapel Hill, NC 27599, USA

³ Department of Computer Science, University of North Carolina at Greensboro, NC 27412, USA

⁴ Department of Statistics and Data Science, School of Management at Fudan University, Shanghai, 200433, China

⁵ Department of Computer Science, University of North Carolina at Chapel Hill, NC 27599, USA

⁶ Department of Genetics, Department of Biostatistics, University of North Carolina at Chapel Hill, NC 27599 USA

⁷ UNC Neuroscience Center, University of North Carolina at Chapel Hill, NC 27599 USA

⁺ Correspondence: Yufeng Liu, Department of Statistics and Operations Research, University of North Carolina at Chapel Hill, 352 Hanes Hall, Chapel Hill, NC 27599, USA.
Email: yfliu@email.unc.edu

* Correspondence: Guorong Wu, Department of Psychiatry, University of North Carolina at Chapel Hill, 343 Medical Wing C, 334 Emergency Room Dr., Chapel Hill, NC 27599, USA.
Email: grwu@med.unc.edu

Word count: 9558

Abstract.

Current diagnostic systems for Alzheimer's disease (AD) rely upon clinical signs and symptoms, despite the fact that the multiplicity of clinical symptoms renders various neuropsychological assessments inadequate to reflect the underlying pathophysiological mechanisms. Since putative neuroimaging biomarkers play a crucial role in understanding the etiology of AD, we sought to stratify the diverse relationships between AD biomarkers and cognitive decline in the aging population and uncover risk factors contributing to the diversities in AD. To do so, we capitalize on a large amount of neuroimaging data from the ADNI study to examine the inflection points along the dynamic relationship between cognitive decline trajectories and whole-brain neuroimaging biomarkers, using a state-of-the-art statistical model of change point detection. Our findings indicate that the temporal relationship between AD biomarkers and cognitive decline may differ depending on the synergistic effect of genetic risk and biological sex. Specifically, tauopathy-PET biomarkers exhibited a more dynamic and age-dependent association with Mini-Mental State Examination scores ($p < 0.05$), with inflection points at 72, 78, and 83 years old, compared with amyloid-PET and neurodegeneration (cortical thickness from MRI) biomarkers. In the landscape of health disparities in AD, our analysis indicates that biological sex moderates the rate of cognitive decline associated with APOE4 genotype. Meanwhile, we find that higher education levels may moderate the effect of APOE4, acting as a marker of cognitive reserve.

Keywords: change point detection, AD biomarkers, dementia risks, sex difference, cognitive reserve

1 INTRODUCTION

Alzheimer's disease (AD) is defined by its underlying pathologic processes that can be measured *in vivo* by imaging biomarkers (Jack et al., 2018; Jack et al., 2013). The most commonly used imaging biomarkers in the research and clinic areas include amyloid β (A β) deposition, pathologic tau, and neurodegeneration (such as cortical thickness), which constitute the backbone of A-T-[N] research framework of AD (Jack et al., 2018). Since AD is clinically heterogeneous in both presentation and progression, converging evidence shows that the one-model-fits-all scenario has limited power to capture the complex relationship between imaging biomarkers and the clinical phenotypes that often demonstrate variable topographic distributions, progression rates, and perhaps underlying mechanisms (Anchisi et al., 2005; Dong et al., 2017b; Lam et al., 2013; Tatsuoka et al., 2013).

It is a common practice to disentangle the heterogeneous population into a set of sub-groups using the clustering technique (Chen et al.; Mu et al., 2023; Mu et al., 2022; Wolk et al., 2009; Young et al., 2018), which stratifies the population based on subject-to-subject biomarker similarities. However, little attention has been paid to characterizing the temporal behavior where the contribution of AD biomarkers to cognitive decline might exhibit diverse trajectories in the long-time course of disease progression. We use the simulated data to demonstrate the importance of stratifying disease progression trajectories and its advantage over existing data clustering methods. As shown in **Fig. 1** (bottom-left), a single linear regression model is limited to capturing the complex relationship between imaging phenotypes and the clinical outcome, where the red, purple, and black axes denote the imaging data, outcome score, and age, respectively. To disentangle the massive data heterogeneity, it is a common practice to first cluster subjects into a set of sub-groups based on the imaging (or omics) phenotypes and then apply the statistical inference to each group separately. As shown in **Fig. 1** (top-left), the statistical power of the current two-step approach is still not strong enough even applying the non-linear statistical model to the stratified groups. Indeed, the problem is rooted in the gap between population stratification and statistical inference, where *the subject-to-subject similarity (drives data*

clustering) does not necessarily align with the brain-to-phenotype relationship. Since the clinical outcome information is not used in the clustering step, the sub-optimal stratification result is responsible for the underpower issue of statistical analysis. In this regard, it is of high demand to investigate the temporal behaviors of the brain-to-phenotype relationship. As shown in the bottom-right of **Fig.1**, the two-stage stratification has significantly improved linear regression performance by jointly detecting the transition of the relationship and applying statistical inference.

In light of this, we sought to uncover the multi-stage mechanism of the A-T-[N] framework by capturing the critical fluctuation (change point) of the biomarker-to-outcome relationship as the cognitive status progressively declines. The concept of our change point detection (CPD) model is shown in **Fig. 2**, which is designed to detect possible changing points in the relationship between imaging biomarkers (between A, T, [N] biomarkers) and MMSE (mini-mental state examination) score (Arevalo-Rodriguez et al., 2015), where biological sex, *APOE4* status, and education level are included as additional covariates in the model. Thus, under the hood of change point detection, our statistical inference model is essentially a spatial-temporal clustering approach on high-dimension neuroimaging biomarkers with a statistical guarantee on the effect size and significance of data-driven findings.

We would like to highlight that the identified change points are not predetermined but are detected using a data-driven process, implemented within our hypothesis testing framework for change point detection. Our CPD model is specifically crafted to pinpoint critical change points in the progression of AD. These change points are characterized by shifts in the relationship between clinical scores and brain imaging along the age of candidates, which in turn signal different stages of AD (Ma et al., 2022). In particular, for each AD biomarker, we first test whether the change point exists and whether multiple change points exist. Next, we project the detected change point to the chronic age axis, which allows us to stratify the diverse progression of AD into a set of distinct stages. On top of identified change points in the progression of AD, we put the spotlight on the multi-factorial mechanism of AD risk disparities (such as biological sex and *APOE4* status)

that contributes to diverse incidence and prevalence of AD. At each identified change point, we investigate the relationship between AD biomarkers and clinical assessment before and after the change point, stratified by males and females, by APOE carriers and non-carriers, and by high-education and low-education, respectively. The secondary analysis is to repeat the main analysis with respect to memory-specific and executive-function-specific composite scores separately.

The output of our analysis provides a novel insight into the diversities and disparities in AD, where the stratified progression stages allow us to disentangle the heterogeneities in AD. Since pre-symptomatic or early symptomatic interventions may ultimately constitute the best long-term therapeutic strategy, the disentangled temporal behavior of cognitive decline offers a new window to manage the priority of risk factors more effectively in AD treatment.

Relevant works. Since AD is a multi-factorial disease (Iqbal and Grundke-Iqbali, 2010), the extant literature supports that there are multiple factors (such as demographic data, genetic risks, and lifestyles) contributing to the heterogeneous trajectories of cognitive decline. In this regard, various clustering approaches have been employed to identify latent sub-groups based on the distribution of neuroimaging data (Dong et al., 2016; Hwang et al., 2016; Jack et al., 2016; Noh et al., 2014). For example, K-median clustering analysis on [¹⁸F]AV-1451 tau-PET data was used to determine how AD subjects vary in the relative involvement of the entorhinal cortex and neocortex (Whitwell et al., 2018), where three subtypes were reported likely corresponding to the postmortem subtypes. Semi-supervised machine learning methods (Dong et al., 2017a) have been applied to ADNI data to elucidate the heterogeneity of neuroanatomical differences between subjects with mild cognitive impairment (MCI), AD, and cognitively normal (CN) individuals, with the focus on establishing neuroanatomical and neuropathological (e.g. amyloid and tau deposition) dimensions in AD and its prodromal stages. Despite the fact that the disease progression in AD often involves dynamic interaction between genetic determinants and environmental exposures (Dunn et al., 2019; Eid et al., 2019;

Elbaz et al., 2007), current clustering-based methods do not take varying progression rates among AD patients into consideration.

Recently, event-based statistical modeling has come to the stage to characterize the progression of AD, which models the transition from normal to abnormal using a set of predefined events (Firth et al., 2020). Such an event-based strategy has been extended to model a more flexible piecewise linear function as well as multiple trajectories for quantifying the progression heterogeneity in AD (Vogel et al., 2021; Young et al., 2018).

Despite a plethora of ways to model the trajectory, current methods often rely on some assumptions about the form of the trajectory function. More critically, longitudinal data with event changes (such as conversion from CN to MCI) are required to infer the parameters in the event-based models. Thus, a limited number of longitudinal data might undermine the potential of event-based approaches in clinical applications. In contrast, our CPD method is designed to characterize the temporal trajectory of neurodegeneration, at a population level, using cross-sectional neuroimages.

Our CPD method effectively models the relationship between AD biomarkers and clinical scores using a linear regression model. In low-dimensional settings where the number of covariates is fewer than the number of observations, change point, and segmentation inference are well-established (Chan et al., 2014; Jin et al., 2013; Maidstone et al., 2017). However, the challenge arises in AD analysis, where data exhibit a high-dimensional structure where the number of biomarkers is larger than the number of observations. In such scenarios, traditional low-dimensional methods are computationally infeasible. Despite recent advancements in high-dimensional change point detection, as explored by (Lee et al., 2016; Zhang et al., 2015), our work presents distinct benefits and differences. Firstly, while existing methods mainly concentrate on estimating the positions of change points, our approach focuses on change point inference. This is achieved by employing bootstrap techniques to maintain the Type I error rate at any given significance level. Therefore, the detected change points have fewer false positives compared to others without statistical inference. Secondly, our CPD method, enhanced with binary segmentation techniques, is adept at detecting and identifying multiple change

points in the regression function. Specifically, once we detect the first significant change point, the algorithm then iteratively examines each half of the data before and after that change point. In each iteration, it looks for evidence of other significant changes in the relationship between clinical scores and AD biomarkers. If a potential change point is detected in a segment, that segment is further divided into two, and the process is repeated for multiple change point detection. This aspect is particularly crucial for modeling the multi-stage neurodegeneration characteristic of AD, setting our method apart in its application and efficacy in AD research.

2 PARTICIPANTS

The data used in our study were obtained from the Alzheimer's Disease Neuroimaging Initiative (ADNI) database (www.ida.loni.usc.edu). ADNI enrolls participants between the ages of 55 and 90 who are recruited at 57 sites in the United States and Canada. After obtaining informed consent, participants undergo a series of initial tests that are repeated at intervals over subsequent years, including clinical evaluation, neuropsychological tests, genetic testing, lumbar puncture, and MRI and PET scans. There are four phases of the ADNI study (ADNI1, ADNI-GO, ADNI2, and ADNI3). Some participants were carried forward from previous phases for continued monitoring, while new participants were added with each phase to further investigate the progression of Alzheimer's disease.

The ADNI data used in this work consists of neuroimaging biomarkers, CSF biomarkers, genetics data, demographic data, clinical outcomes, and socioeconomic status. **Table 1** summarizes the data statistics. Specifically, we collapse the APOE genotype into two subgroups: (1) subjects carrying any ε4 alleles (homozygous ε4/ ε4 and heterozygous ε4/-) and (2) subjects with no ε4 risk alleles (-/-). Hence, the APOE genotype serves as a binary variable in our study (carrier and non-carrier). We adopt the CSF p-tau/Aβ₄₂ ratio

(Campbell et al., 2021) as the CSF hallmark in the following analysis, where higher CSF tau/A β ₄₂ indicates a higher risk of developing AD.

Regarding neuroimaging data, we follow the Destrieux atlas (Destrieux et al., 2010) and use our in-house analytic pipeline based on *FreeSurfer* (Fischl, 2012). Major image processing steps include (1) noise reduction and bias correction on T1-weighted MRI, (2) skull striping, (3) tissue segmentation, (4) cortical surface reconstruction, (5) spatial image alignment which warps the atlas as well as the corresponding label information to the underlying subject space. The output is a whole-brain parcellation that includes 148 cortical regions and 12 sub-cortical structures. After that, we register PET image to the T1-weighted MR image. Based on the Destrieux parcellation, we calculate regional SUVR (Standard Uptake Value Ratio) from amyloid, tau, and FDG-PET scans and obtain the whole-brain A, T, [N] imaging biomarkers, respectively, which are normalized by using the whole cerebellum as the reference region.

The MMSE score is provided in ADNI as one of the major clinical outcomes, which has been widely used as a cognitive screening tool to assess various cognitive functions, including orientation, memory, attention, language, and visuospatial skills (Clark et al., 1999). Specifically, we put the spotlight on the effect of AD-related pathology on memory decline and executive function (EF) decline, respectively. It is worth noting that we derived composite scores for memory decline and EF decline using data from the ADNI neuropsychological battery using item response theory (IRT) methods. The formation of ADNI-MEM was complicated by the use of different word lists in the Rey Auditory Verbal Learning Test (RAVLT) and the ADAS-Cog, and by Logical Memory I data missing by design (Gibbons et al., 2012).

3 METHODS

Principle of change point detection. The primary goal of our CPD methodology is to identify the latent transition points, indicating shifts in the multi-stage progression of relationships between biomarkers and clinical outcomes. By stratifying subjects temporally (e.g., by age), our CPD method seeks to statistically test

the significance of these temporal transitions in relation to the aforementioned relationships. Specifically, let

$(Y_i, X_i)_{i=1}^N$ be N chronically ordered independent realizations of (Y, X) by another variable Z , such as age.

We employ a linear regression model $Y_i = \mathbf{X}_i^T \boldsymbol{\beta} + \varepsilon_i$ to fit the relationships between p -dimensional biomarker data \mathbf{X}_i and clinical outcome Y_i . Here, $\boldsymbol{\beta}$ represents the p -dimensional unknown vector of coefficients, and ε_i is the error term. Our objective is to test whether the regression coefficients $\boldsymbol{\beta}$ that describe the regression plane of $Y \sim \mathbf{X}$ has a change point among the observations. Let $\boldsymbol{\beta}^{(1)}$ and $\boldsymbol{\beta}^{(2)}$ be two p -dimensional vectors of coefficients. We consider the following linear regression model with a potential change point:

$$Y_i = \mathbf{X}_i^T \boldsymbol{\beta}^{(1)} + \varepsilon_i, \quad \text{if } Z_i \leq a^*;$$

$$Y_i = \mathbf{X}_i^T \boldsymbol{\beta}^{(2)} + \varepsilon_i, \quad \text{if } Z_i > a^*.$$

Here, a^* represents the position of the change point on the range of Z . If Z is specified as the ages of objectives, then for those subjects that are younger than a^* , the relationship between $Y \sim \mathbf{X}$ is characterized by $\boldsymbol{\beta}^{(1)}$, while for subjects that elder than a^* , the relationship is captured by $\boldsymbol{\beta}^{(2)}$. In this case, a^* serves as the critical change point that we aim to detect, marking a significant transition in the biomarker-to-outcome relationship. This change is crucial to detect in the context of AD progression.

Our CPD model aims to identify and estimate this specific time point where there's a significant shift between the regression models before and after that moment. We consider the following hypothesis testing framework:

$$H_0: \boldsymbol{\beta}^{(1)} = \boldsymbol{\beta}^{(2)} \text{ for all } a, \text{ vs. } H_1: \boldsymbol{\beta}^{(1)} \neq \boldsymbol{\beta}^{(2)} \text{ for specific } a^*.$$

In other words, under H_0 , the regression coefficients are homogeneous across all observations, while under H_1 , there is a change point at an unknown time point a^* , resulting a sudden shift in regression coefficients after a^* . By conducting statistical inference based on the above hypothesis testing framework, our CPD model can provide a p -value using bootstrap to describe the significant level of the detected change point (van

de Geer et al., 2014). A significant p -value leads to the rejection of null hypothesis, thereby supporting the existence of a change point. Then, our second goal is to estimate the change point location when we conclude the existence of the change point. By adopting the hypothesis testing framework, one of the advantages of our approach is the reduced risk of detecting false positives in change points, making the methodology more robust and reliable for applications in clinical research.

Integrated solution of change point detection. The methodology of our CPD model is structured into four main steps, enabling the identification of significant transition points in the progression of relationships:

Step 1: High Dimensional Regression Analysis. We start by discretizing the time domain into n segments. For each potential cut point, de-biased lasso estimators are computed to model the relationship before and after the cut point. This step is crucial in setting the groundwork for identifying possible transition points in the data.

Step 2: Change point detection. Next, we employ an argmax-based change point estimator (Liu et al., 2023). This involves synthesizing information from various potential change point locations. The underlying rationale is that the largest discrepancy in model coefficients should manifest at the actual transition point, indicating a significant shift in the data's behavior.

Step 3: Bootstrap. Bootstrap techniques are then utilized to assess the significance of the statistics obtained from the previous step. This analysis yields a p -value, which is critical for the hypothesis testing process. It helps in determining the statistical significance of the identified change points.

Step 4: Multiple change point detection. Finally, our model incorporates a refitting step combined with a binary segmentation technique, an approach conducive for detecting multiple change points (Fryzlewicz, 2014). This recursive process involves iteratively examining each data segment pre and post the initial change point. If subsequent significant change points are detected within a segment, the segment is further split, and the process is reiterated. This iterative approach is particularly adept at unraveling the multifaceted stages of AD progression.

If the p -values for each binary split are significant, the CPD algorithm outputs the precise locations of the change points along with regression estimations for each identified time period. This comprehensive detection mechanism offers a nuanced understanding of the multiple stages in AD progression (Liu et al., 2021, 2022; Liu et al., 2020), which is pivotal for informed clinical decision-making and targeted therapeutic interventions (Liu et al., 2021, 2022; Liu et al., 2020).

3 RESULTS

In this section, we delve into the results of our AD analysis. We start with simulation studies that serve as a precursor to real data application. In Section 4.1, we intricately design the simulation settings to replicate the complexities of AD analysis, serve as a critical preliminary test for our CPD method. The primary objective here is to evaluate the robustness and sensitivity of the method. These simulations yield promising outcomes, showcasing the method's effectiveness in accurately identifying and locating change points, which demonstrates a testament to its potential in analyzing AD degeneration.

With this strong simulation-based foundation, we transit to real data analysis in the subsequent sections. Here, we apply our CPD method to key AD biomarkers: A, T, and [N]. In Section 4.2, we spotlight a significant revelation: the Tau biomarker is more sensitive than A and [N] in monitoring cognitive decline. This critical finding, marked by the detection of multiple significant change points in Tau linked to AD degeneration, naturally shifts our analytical focus toward Tau in the following analysis.

Progressing to Sections 4.3 and 4.4, we focus on interpreting the changes detected by the Tau biomarker at each identified change point in AD progression. This exploration is enriched by considering important biomarkers, such as biological sex and *APOE4* status. These factors are crucial, as they offer insights into the biomarkers' differential impacts across diverse individual's profiles. Further broadening our analysis in

Section 4.5, we incorporate socioeconomic factors, such as education level, into our study. This inclusion acknowledges the potential influence of social determinants on the progression of AD, adding depth to our understanding of AD progression.

Finally, in Section 4.6, we confront the multifaceted nature of cognitive decline in AD. By dissecting the global MMSE score into Memory (MEM) and Executive Functioning (EF) composite scores, we strive to disentangle the complex, time-dependent interactions between AT[N] biomarkers and these specific cognitive domains. The analysis on splitting the MMSE score not only provides insights on the varied clinical presentations of AD but also enhances our comprehension of its progression.

4.1 Sensitivity and robust analysis.

To test the stability and robustness of our CPD method, we conduct the following comprehensive simulation studies. These studies are designed to encapsulate three distinct cases: (1) No change point case; (2) Single change point detection; (3) Multiple change point detection. For the design matrix \mathbf{X} , we generate i.i.d \mathbf{x}_i that follows multivariate normal distribution $N(0, \Sigma)$ where $\Sigma = (\sigma_{i,j})_{i,j=1}^p$ and $\sigma_{i,j} = 0.5^{|i-j|}$. The error terms ε_i 's are i.i.d. generated from standard normal distributions. To mimic the real data, we choose age as the sorting variable Z , represented in years, and generated it from a truncated normal distribution $N(75, 10)$ within the interval [50, 100]. In the regression model, the first five covariates are assigned with non-zero coefficients, while the coefficients of the remaining $p - 5$ covariates are set to zero. These non-zero coefficients are independently and identically drawn from a uniform distribution $U(0, 2)$.

In the no change point case, we maintained a uniform regression function across all observations, characterized by a single set of regression coefficients $\boldsymbol{\beta}^{(1)}$. For the single change point case, the true regression function was designed to change for subjects older than 75 years old. We add a signal jump $\delta =$

$\sqrt{\frac{\log(p)}{n}}$ to the 5 non-zero covariates of $\boldsymbol{\beta}^{(1)}$ to generate $\boldsymbol{\beta}^{(2)}$. For the multiple change point case, we

consider three change points at ages 70, 75, and 80 years old. The above three change points divide the data

into four segments, each with distinct regression coefficients: $\beta^{(1)}$, $\beta^{(2)}$, $\beta^{(3)}$, and $\beta^{(4)}$. At each change

point, a signal jump $\delta = \sqrt{\frac{\log(p)}{n}}$ is introduced to the non-zero covariates, ensuring a systematic shift in the

dataset's underlying structure. This underlying structure of regression model tends to mimic the multi-stage degeneration of AD.

For tuning parameter selection of de-biased lasso in Step 1 of our CPD method, we apply 5-fold cross-validation using mean square error as the evaluation metric. To assess the method's robustness and sensitivity, we vary the sample size from 500 to 1000 and increase the dimension of covariates from 100 to 200. The number of bootstrap replications for statistical inference is set at $B = 100$, with a significance level of 0.05. All numerical results in above three cases are based on 50 replications. Our hypothesis testing aims to demonstrate that (1) no significant change point should be detected in the first case, (2) a single significant change point close to the age of 75 should be detected in the second case, and (3) three significant change points around 70, 75, and 80 years should be detected in the third case.

As shown in **Table 2**, for the no change point case, nearly all combinations of sample size and covariate dimensions yield non-significant p-values, indicating a low risk of false positives for change point detection. In the single change point case, significant p-values (0.00) are consistently returned, with the estimated change point closely approximating 75 years and exhibiting small standard errors, affirming our method's accuracy even when we reduce sample sizes to 500 and increase dimensions to 200. **Fig. 3** showcases the density plots for the detected change points across multiple scenarios. Notably, the plots feature three distinct peaks, each corresponding to the true change points identified at ages 70, 75, and 80. This clear delineation of peaks at the specific ages reinforces the accuracy of our CPD method in pinpointing the precise moments of transition in the regression function. Even under conditions of smaller sample sizes and higher dimensions, our method successfully identifies these change points with a high degree of probability. This consistent detection of key

transition ages in the plots underscores the robustness and reliability of our CPD approach, particularly in its capability to detect multiple stages in AD progression.

4.2 Tau biomarker is more sensitive to monitoring cognitive decline than A and [N] biomarkers

Building on the foundation of the simulation analysis, we transition to real data analysis, applying our CPD method to distinct biomarkers: Amyloid (A), Tau (T), and Neurodegeneration [N]. The change point detection results for A~MMSE, T~MMSE, and [N]~MMSE are summarized in **Table 3**. The relationship between T and MMSE appears to have three critical transition points at the ages of 72, 78, and 83. When compared to A-Biomarker, which shows no significant change point in the 55-97 age range, the temporal relationship between T and MMSE is more heterogeneous, displaying multiple progression stages. As shown in **Fig.4(a)**, the strongest change point in the T~MMSE relationship occurs at 78 years old, with the largest difference in slope between the two linear models. At a significant level of $p < 0.001$, a one-unit increase in tauopathy burden results in a 1.13 decrease in MMSE score before the age of 78 (left panel in **Fig. 4(b1)**). However, after age 78, the decline becomes much more rapid, with a one-unit increase in tauopathy burden leading to a 2.44 decrease in MMSE score (right panel in **Fig. 4(b1)**). To substantiate the significant temporal shift in the T-biomarkers relationship after age 78, we further execute a z-test specifically aimed at comparing the regression coefficients of the whole brain Tau SUVR. The resulting p -value, calculated to be 0.03, aligns coherently with the significant differences highlighted by our CPD model. Additionally, the second and third significant change points occur at the ages of 72 and 83, respectively. The fitted linear relationships between the T-biomarker and MMSE score are displayed in **Fig. 4(b2)** for three age ranges: before 72, between 72 and 83, and after 83, where T-biomarkers are closely correlated with MMSE score ($p < 0.001$). In contrast, the p -value of 0.38 obtained from the z-test on the whole brain A-biomarker indicates that, the decline slopes due to A-biomarker do not manifest a significant difference before ($\beta = -1.25$) and after ($\beta = -0.74$) the identified change point (age 77), albeit the A-biomarkers show a strong correlation to MMSE score ($p < 0.001$) both before and after change point (**Fig. 5(a)**).

In **Fig. 5(b)**, we demonstrate the fitting error using a global linear regression model (in red) and a piecewise linear regression model (in green) that leverages the identified change points. It is evident that using piecewise line fitting has reduced the T-MMSE fitting error by 6.3% in terms of the residual between observed MMSE and linearly-fitted MMSE scores, suggesting the importance of stratifying the temporal heterogeneity of T-MMSE in disease progression.

Remarks. Since AD biomarkers consist of regional SUVRs from 160 brain regions, we use the whole-brain average as a global measurement to quantify their collective impact on MMSE score (as shown in **Fig. 4(b)** and **Fig. 5(a)**). To identify the brain regions that have the most significant impact on the occurrence of changing points, we utilize a fused LASSO model (Tibshirani, 1996) to select a collection of brain regions that make the largest contribution to the changing points underlying the T-MMSE relationship. The fusion penalty helps to penalize the spurious difference of the regression coefficients for each covariate across the estimated stages (Arnold and Tibshirani, 2016). From left to right, we display the selected brain regions that are associated with critical transition ages 72, 78, and 83 in **Fig. 6(a)**, where the node size is proportional to the impact level. The summary of these brain regions is listed in **Fig. 6(b)**.

4.3 Main effect of biological sex and *APOE4* status in T-MMSE relationship

To deepen our understanding of AD progression, we focus on interpreting the relationships between AD biomarkers and clinical assessments at each identified change point in Tau. We start by considering variations across important biomarkers: biological sex and *APOE4* status. In piecewise linear regression model of T-MMSE relationship, we found that the effect size of both biological sex and *APOE4* status are significant ($p < 0.05$). In this context, we sought to examine the stratified T-MMSE relationship for sex and *APOE4* status separately. Due to the clinical significance of the age of 72 and 78 as the top two critical transition points in the T-MMSE relationship for early prevention of AD, we further apply the linear regression model before and after the change point for males and females (**Fig. 7**) and *APOE4* carriers and non-carriers (**Fig. 8**), respectively.

Our analysis reveals notable gender-specific differences in the progression of cognitive decline associated with whole brain Tau SUVR prior to the identified change point at age 78. Stratifying the data by gender, we observed a marked disparity in the regression coefficients before the age of 78: a *z*-test yielded a *p*-value of 0.019, indicating a significant difference between genders. Specifically, for females, a one-unit increase in whole-brain tau burden corresponds to a 1.57 unit decrease in the MMSE score before age 78, in stark contrast to a 0.45 unit decrease observed in males. This suggests a more rapid cognitive decline in females compared to males in the pre-78 age group. Interestingly, after age 78, this decline in cognitive function becomes more uniform across genders, as indicated by a *p*-value of 0.27. This convergence in decline rates after the age of 78 implies a diminishing gender disparity in the progression rate at later stages.

Additionally, our stratification analysis based on APOE4 status reveals a universally steeper decline slope in APOE4 carriers as compared to non-carriers, with a significant *p*-value of 0.039 observed before the age of 78. This finding suggests that APOE4 is a significant risk factor for AD progression, with carriers being at a higher risk than non-carriers for more rapid cognitive decline.

4.4 Sex-dependent APOE effect on cognitive decline

Along with current findings in AD (Altmann et al., 2014; Andrew and Tierney, 2018; Barnes et al., 2005; Davis et al., 2021), our results in **Fig. 7** and **Fig. 8** indicate that, in the early stages of Alzheimer's Disease, there appears to be a more rapid cognitive decline in women compared to men, and APOE4 carriers seem to experience a more pronounced decline than non-carriers. In this regard, we sought to investigate how the mechanistic role of AD biomarkers changes in mediating the effect of *APOE4* on the cognitive decline before and after the change point. We follow the classic mediation analysis to estimate the direct effect β_D (DE) and mediation effect β_M (ME) for the mechanistic pathways of *APOE4*→MMSE and *APOE4*→AD biomarker→MMSE, respectively.

Mediation analysis for T-biomarker prior to and after the age of 78 (1st change point).

Firstly, we examine the direct pathway of *APOE4* affecting MMSE score and the indirect pathway that is mediated by whole-brain T-biomarker (average of tau SUVRs across 160 brain regions). At a significant level of 0.01, *APOE4* significantly contributes to the decrease of MMSE score via the increase of whole-brain tau aggregates (shown in **Fig. 9(a)**). Prior to the change point (age of 78), the estimated β_D and β_M are -0.01 and -0.18, respectively, with the indirect pathway accounting for 94.6% proportion of the effect on the decrease of MMSE score. However, after the change point, both direct and indirect pathways equally affect cognition, with the proportion between DE ($\beta_D = -0.26$) and ME ($\beta_M = -0.27$) balanced at 50.8%. It is apparent that (1) the risk associated with *APOE4* becomes more pronounced as age advances, and (2) there is a noteworthy transition from a ME-dominant pattern of *APOE4* effect on the cognitive decline to the neurodegeneration pattern where the direct and indirect pathways are more evenly balanced.

Secondly, we sought to investigate the driving factor behind such pattern shifts before and after the change point. We hypothesize that the change in the ME/(ME+DE) proportion from 94.6% to 50.8% is sexually dimorphic. To do so, we stratify the same medication analysis to males and females, as shown in **Fig. 9(b)**. Specifically, our findings indicate that the cognitive decline in female *APOE4* carriers is consistently influenced by the accumulation of tau aggregates in the whole brain, as evidenced by the ME/(ME+DE) proportions of 84.9% before the age of 78 and 97.1% after the age of 78. On the contrary, the ME/(ME+DE) proportion in males decreases from 98.1% to 20.8%, showing that (1) the impact of *APOE4* risk factor on cognitive decline is primarily mediated by the whole-brain tau aggregates in both males and females prior to the change point, (2) male *APOE4* carriers experience a significant shift from the indirect pathway ($\beta_M = -0.15$) to the direct pathway ($\beta_D = -0.39$) after the change point. This piece of evidence suggests that *APOE4* may have a sex-specific effect on the cognitive decline that changes over time.

Thirdly, we localize the mediation analysis by replacing the whole-brain tau aggregation level with regional SUVR. Among 160 brain regions, 4.4% of regions exhibit more than a 100% decrease in ME/(ME+DE) ratio after the change point, and 53.1% of regions exhibit more than a 50% decrease in ME/(ME+DE) ratio after the

change point. The table in the middle of **Fig. 9(c)** presents the mediation effect β_M in nine top-ranked brain regions, sorted in a decreasing order based on the amount of mediation effect β_M before and after age 78. This result indicates that the temporal changes in the way how *APOE4* affects cognitive decline might be region selective. In **Fig. 9(c)**, we display the top nine brain regions where the mediated effect of *APOE4* on cognitive decline (via regional tau SUVR) significantly decreases after the change point (indicated by region size). Furthermore, we color these selected brain regions with respect to the topological location in large-scale functional brain networks (color notation shown at the bottom of **Fig. 9(c)**). It is apparent that the brain regions experiencing significant ME/(ME+DE) proportion transition of *APOE4* effect are located in subcortical areas (purple) and default-mode network (dark blue), which indicates the region-selective pattern in terms of the topological location underlying functional networks.

Fourthly, we sought to identify brain regions that manifest sex differences in terms of changes in medication effect before and after the change point, by combining the male/female stratification analysis on top of the regional mediation analysis of *APOE4*→Tau→MMSE pathways. At the significance level of $p < 0.05$, we have not detected any brain region exhibiting a significant change in the proportion of mediation effects before and after age 78 in the stratification analysis between males and females.

Mediation analysis for [N]-biomarker prior to and after the age of 72 (1st change point).

Since age 72 is the only significant change point detected in [N]~MMSE relationship, we investigate the mechanistic role of [N] biomarker in regulating the effect of *APOE4* on cognitive decline. The major findings of mediation analysis in the *APOE4*→FDG→MMSE pathway are summarized below.

- We found that only 38.2% of *APOE4* effect on the decrease of MMSE has been mediated by the decrease of whole-brain metabolism level (approximated by the average of regional FDG-SURVs) before the change point (shown in **Fig. 10(a)**), at a significant level $p < 0.01$. After the age of 72, the ME portion is further reduced to 15.4%, indicating that the *APOE4* risk factor exerts a direct effect on cognitive decline underlying the *APOE4*→[N]→MMSE pathway.

□ We found that both men (from 42.9% before age 72 to 15.8% after age 72) and women (from 35.3% before age 72 to 15.9% after age 72) contribute to the decline of ME/(ME+DE) proportion prior to and after the change point, as shown in **Fig. 10(b)**.

□ We conduct the same mediation analysis for each brain region. Our findings indicate that 7.5% of regions exhibit more than a 100% decrease in ME/(ME+DE) ratio after the change point, and 60% of regions exhibit more than a 50% decrease in ME/(ME+DE) ratio after the change point. In this context, it is possible that the role of [N] biomarkers in the APOE4→[N]→MMSE pathway undergoes temporal changes that are specific to certain regions at the change point. The top eleven brain regions with the largest decrease in ME/(ME+DE) ratio before and after the change point are displayed in **Fig. 10(c)**, where the before vs. after mediation effects β_M as well as the significance levels are listed in the middle of **Fig. 10(c)**. In general, most of the top-ranked brain regions are located in the default mode network.

□ On top of the regional mediation analysis in **Fig. 10(c)**, we further stratify the statistical tests into males and females separately. In the middle of **Fig. 10(d)**, we first display the brain regions where the proportion of medication effects manifest significant change before and after age 72 in both males and females, at a significance level of $p < 0.01$. It is evident that most of the brain regions in the default mode network manifest the change of mediation role by the reduced metabolism level. This temporal pattern is observed in both males and females. Second, male-specific and female-specific brain regions that exhibit the same temporal changing patterns are displayed in **Fig. 10(d)** left and right, respectively.

4.5 Role of socioeconomic status in modifying multi-stage progression of AD biomarkers

Multiple lines of findings have reported that socioeconomic status significantly modifies the progression of AD. In our change point detection model, we found that education level also manifests a significant association in the multi-stage T~MMSE and [N]~MMSE relationships. Hence, we stratify the statistical analysis underlying the T~MMSE relationship for the low education group (less than 16 school years) and high education group (more than 16 school years) at the age of 78 (most critical change point).

Impact of education level on T-MMSE relationship prior to and after the age of 78.

Firstly, we found that both low and high-education groups exhibit a moderate-to-rapid decline pattern before and after the change point, as shown in **Fig. 11(a)**. Using the significant level $p < 0.05$, the decline in the low-education group (-1.65 before age 78 and -2.88 after age 78) is more severe than that in the high-education group (-0.99 before age 78 and -2.03 after the change point).

Secondly, we examine the direct and indirect effects along the $APOE4 \rightarrow T \rightarrow MMSE$ pathway. For the high-education group (**Fig. 11(b)** top), the proportion of the mediation effect of *APOE4* on MMSE decreases from 95.2% to 21.6% after age 78. On the contrary, the low-education group shows the opposite pattern, where the proportion of mediation effect of *APOE4*, $ME/(ME+DE)$, on MMSE increases from 59.7% to 76.1% after age 78. This observation implies that education level could be a modifying factor in the pathophysiological mechanism underlying the impact of *APOE4* risk factor on cognitive decline. Since education level has been found to be a strong predictor of cognitive reserve (Stern, 2012), we provide an in-depth discussion in **Section 5**.

Impact of education level on [N]-MMSE relationship prior to and after the age of 72.

Similarly, we investigate the role of education level in $[N] \sim MMSE$ relationship before and after age 72 (the only change point). At a significance level $p < 0.001$, the reduced metabolism level (measured by whole-brain concentration level from FDG-PET scan) shows increased effect size (1.44 prior to age 72 and 1.61 after age 72) in the low education group (**Fig. 12(a)** top). However, the high education group manifests an opposite changing pattern where the effect size of a unit decrease of metabolism level is associated with a 1.49 unit decrease of MMSE score before age 72 while reduces to a 1.28 unit decrease of MMSE score after the change point (**Fig. 12(a)** bottom).

At a significance level of $p < 0.05$, the mediation analysis results in **Fig. 12(b)** top suggest that high education group exhibits a more profound indirect pathway prior to the age 72 (i.e., the majority of *APOE4* effect on cognitive decline is mediated by the reduced whole-brain metabolism level), where the proportion of

medication effect can reach 79.8%. After the change point, however, there is a pronounced change in the high education group that the effect of *APOE4* on cognitive decline shifts to the direct pathway, as indicated by the drop of the proportion of medication effect to 15.8%. Regarding the medication analysis of *APOE4*→[N]→MMSE pathway in low-education group (**Fig. 12(b)** bottom), our finding suggests that *APOE4* effect on cognitive decline is primarily driven by the direct pathway. Furthermore, we observed a moderate change in the proportion of the mediation effect, with a decrease from 27.1% before the age of 72 to 16.5% after the age of 72.

4.6 Multi-stage association between cognitive composite score and AD hallmarks

Cognitive function is complex and multidimensional, which is partially responsible for the heterogeneous clinical manifestations reported in the progression of AD. In this regard, we sought to break the global MMSE score into MEM and EF composite scores and disentangle the temporal heterogeneity underlying the relationships of AT[N] biomarker~MEM (in **Table 4**) and AT[N] biomarker~EF (in **Fig. 13**), respectively.

Firstly, we have detected one change point underlying A~MEM relationship at the age of 74, one change point underlying [N]~MEM relationship at the age of 74, and two change points underlying T~MEM relationship at the ages of 80 and 86. However, none of the change points in the A~MEM, T~MEM, and [N]~MEM relationship pass the statistical significance test at the significance level of $p < 0.05$ (shown in **Table 4**). This finding suggests that the linear effect of AT[N] biomarkers on memory performance does not show significant change over time.

Secondly, we found that AT[N] biomarkers exhibit a multi-stage impact on the decline in EF performance (shown in **Fig. 13a**). Using a significant level of $p < 0.001$, we identified two change points underlying A~EF relationship: the first occurs at the age of 70, followed by a second change point at the age of 76. T~EF relationship shows two change points occurring at the age of 79 and 86, respectively. However, the second change point (86-year-old) is not significant. There is only one statistically significant change point in the [N]~EF relationship occurring at the age of 72. These findings suggest that the effect of AT[N] biomarkers on

EF performance is much more dynamic than AT[N]~MEM relationship. From **Fig. 13b** to **Fig. 13d**, we display the brain regions on which the regional A, T, and [N] burdens have a significant impact on the decline of EF performance (The node size is proportional to the effect size). Furthermore, we localized these brain regions in the context of large-scale functional brain networks. We found that (1) most brain regions underlying A~EF relationship are located in the left hemisphere, (2) the accumulation of tau aggregates in the default mode network is associated with the multi-stage T~EF relationship, (3) the decreased metabolism levels in the sub-cortical area and visual cortex underline the temporal change of [N]~EF relationship.

5 DISCUSSION

Multi-stage relationship between imaging biomarkers and the CSF biomarkers. In addition to sorting the change points based on the chronicle ages, it is straightforward to identify change points and sort in other continuous AD-related variables, such as CSF biomarkers. In **Fig. 14**, we demonstrate the application of disentangling the latent multiple stages in the evolving [N]~MMSE relationship as the accumulation of CSF biomarkers. Since it is common to use the CSF tau/A β_{42} ratio in clinical practice, we adopted the CSF tau/A β_{42} ratio as the sorting variable, where a larger CSF tau/A β_{42} indicates a higher risk of developing AD. Therefore, each subject has a collection of 160 regional [N] biomarkers from the FDG-PET scan, MMSE score, and the CSF tau/A β_{42} biomarker. As shown at the top of **Fig. 14**, the first (most critical) change point in the [N]~MMSE relationship occurs at the early stage of CSF biomarker accumulation ($\text{tau}/\text{A}\beta_{42} = 0.37$), followed by the second and third change points occurring at $\text{tau}/\text{A}\beta_{42} = 0.61$ (middle stage of AD progression) and $\text{tau}/\text{A}\beta_{42} = 0.89$ (late stage of AD progression). In **Fig. 14** bottom, we display the brain regions on which the reduced metabolism level has a strong contribution to the change of the linear relationship between [N] biomarker and MMSE score.

Clinic impact of our work. AD is the most common form of dementia that affects older people of varying ethnicities, sexual and gender identities, and lifestyles (Organization, 2012). The heterogeneity in the

presentation and progression of clinical symptoms poses great challenges to fully elucidating the complex interaction between disparities and diversities in AD. In this regard, an in-depth understanding of health disparities will set the stage for the development of precision medicine in AD by encompassing personalized strategies for prevention, detection, drug development, and disease-modifying therapy. Specifically, the identified change points in AD progression would be beneficial for (1) a comprehensive underpinning of the interaction between health disparities and cognitive change over time that might provide practice guidelines for analyzing and understanding diversities in drug development and disease-modifying therapeutics for AD, (2) a new neurobiological mechanism that links biological indicators with environmental exposures which provides an in-depth understanding of health disparities in AD, and (3) a more effective health care system that is accessible and equal for all Americans, regardless of gender, race, ethnicity, geography, and socioeconomic status.

In this work, we investigate the synergistic effect of APOE4 and biological sex on the diversities of cognitive decline in AD, with the focus on (i) common and distinct dynamic patterns of disease progression across amyloid (A), tau (T), and neurodegeneration (N) biomarkers (**Fig. 4**, **Fig. 5**, and **Fig. 6**), (ii) sex-dependent effect of *APOE4* status on the long period of neurodegeneration (**Fig. 7-10**), and (iii) the protective factors behind the health disparities at the different stages of AD (**Fig. 11** and **Fig. 12**).

Education, a marker of cognitive reserve, is protective against cognitive decline. Education has long been recognized as an important indicator of greater cognitive reserve, which is the brain's ability to compensate for age-related brain changes and greater neuropathological burden (Stern, 2006, 2012). In our study, the impact of APOE4 on cognitive decline was found to be moderated by level of premorbid education (**Fig. 11b** top), where the total effect size (DE+ME) of *APOE4* are -0.04 before age 78 and -0.27 after age 78 , compared to low education group (**Fig. 11b** bottom), where the total effect of *APOE4* are -0.39 before age 78 and -0.57 after age 78. This suggests that education may provide a cognitive 'buffer' that helps to delay the onset of AD.

These findings underscore the importance of lifelong learning and the value of education in promoting healthy aging and maintaining cognitive function in old age.

Limitation of current work and future direction. There are several methodology and application-wise limitations in our current approach. In the following, we discuss each limitation and possible solutions.

1. Cross-sectional vs. longitudinal. Our current CPD method is designed for modeling the population-wise change of neurodegeneration trajectory from cross-sectional data. Specifically, we simultaneously stratify the subjects in the temporal domain (by age) and test whether the temporal transitions show statistical significance in terms of the biomarker-outcome relationship. Since subject-specific changes are oftentimes more relevant to disease progression, future work should take subject-specific longitudinal change into account by integrating the mixed-effect model into our CPD method.
2. Normal aging v.s. highly selective disease data. The data analysis in this work used ADNI data only, which is a clinical research study in AD. However, the presence and incidence of AD might not be accurately reflect the general aging population in the clinic routine. To address this issue, our future work includes extending the data analysis to multi-site studies by exploring other public datasets such as Biocard (Sacktor et al., 2017) and UK Biobank (Fawns-Ritchie and Deary, 2020).
3. *Multi-factorial mechanisms of health disparities in AD.* Since AD is a multi-factorial disease (Iqbal and Grundke-Iqbali, 2010), the extant literature supports the hypothesis that there are multiple factors contributing to the presence of diverse disease progression in the aging population. However, little attention (including our work) has been given to understanding their relationship and how their interaction affects the trajectory of cognitive decline. For example, *APOE4* risk tends to vary by race. Although it is important to examine whether race plays a role, the majority body of recruited subjects in ADNI are genetically related to European ancestry. In this regard, our work is unable to detect race

differences. Advanced multivariate statistical models are in high demand to elucidate the synergistic effect of phenotypic variables on the progression of AD.

4. *Cognitive reserve in AD prevention.* A major challenge in the care and management of AD is the paradoxical relationship between the burden of AD pathology and its clinical outcome (Stern, 2002; van Loenhoud et al., 2019). Recent evidence shows cognitive reserve, the brain's capability to preserve cognition despite underlying AD pathology, is a key determinant that moderates clinical progression (Medaglia et al., 2017; Reed et al., 2010; Stern, 2002, 2006, 2012, 2017; van Loenhoud et al., 2019; van Loenhoud et al., 2017). Following this notion, we investigate the role of education level in change points, and we find that greater education might buffer against cognitive decline. While education level is thought to be an important marker of cognitive reserve, other markers, including premorbid verbal IQ, occupational complexity, and others have also been suggested as providing important proximal markers of this complex construct (Stern et al., 2020). Future studies may therefore, benefit from the incorporation of additional measures of cognitive reserve to more comprehensively assess this protective factor.

5. *Extend from AT[N] to ATX[N] framework.* The AT[N] framework (Jack et al., 2018) is the most popular AD research framework that characterizes individuals using amyloid- β pathway (A), tau-mediated pathophysiology (T), and neurodegeneration biomarker (N). Our current work follows the AT[N] framework. Recently, the biomarker matrix has been expanding to an ATX[N] system (Hampel et al., 2021), where X represents novel candidate biomarkers such as neuroimmune dysregulation, synaptic dysfunction, and blood-brain barrier alterations. Upon the availability of new biomarker data in the public database, it is worthwhile to investigate the temporal behaviors of X biomarkers in the aging population.

6 Conclusions.

Our findings provide critical refinements that delineate previously undifferentiated heterogeneity within AD progression using a powerful multi-variate statistical model of change point detection. Our investigation focused on the multi-stage progression between AD biomarkers and clinical phenotypes. Our findings extend prior work demonstrating differential associations between AD biomarkers and clinical decline by showing that the T-biomarker exhibits more change points than the A and [N] biomarkers as cognition declines during AD progression. We also observed that genetic risk (i.e. APOE4), biological sex, and cognitive reserve exert important influences on the transition from AD biomarker elevations to clinical phenotypes. Our results highlight the critical importance of delineating individual differences influencing the impact of AD biomarkers to clinical phenotype.

It is important to recognize that understanding differential risks and rate of AD progression is a critical challenge in the development of precision medicine for the disease. Personalized strategies for prevention, detection, drug development, and disease-modifying therapy can only be effective if they take into account the complex interactions between health disparities and cognitive change over time. Our data-driven approach can help achieve this goal in several ways. *Firstly*, it can provide a comprehensive understanding of the impact of health disparities on cognitive change over time, which can be used to develop practice guidelines for analyzing and understanding diversities in drug development and disease-modifying therapeutics for AD. *Secondly*, our approach can reveal new neurobiological mechanisms that link biological indicators with environmental exposures, providing a more in-depth understanding of health disparities in AD. *Thirdly*, our findings can inform the development of a more effective healthcare system that is accessible and equitable for all Americans, regardless of gender, race, ethnicity, geography, or socioeconomic status.

Acknowledgments

Data collection and sharing for this project was funded by the Alzheimer's Disease Neuroimaging Initiative (ADNI) (National Institutes of Health Grant U01 AG024904) and DOD ADNI (Department of Defense award number W81XWH-12-2-0012). ADNI is funded by the National Institute on Aging, the National Institute of Biomedical Imaging and Bioengineering, and through generous contributions from the following: AbbVie, Alzheimer's Association; Alzheimer's Drug Discovery Foundation; Araclon Biotech; BioClinica, Inc.; Biogen; Bristol-Myers Squibb Company; CereSpir, Inc.; Cogstate; Eisai Inc.; Elan Pharmaceuticals, Inc.; Eli Lilly and Company; EuroImmun; F. Hoffmann-La Roche Ltd and its affiliated company Genentech, Inc.; Fujirebio; GE Healthcare; IXICO Ltd.; Janssen Alzheimer Immunotherapy Research & Development, LLC.; Johnson & Johnson Pharmaceutical Research & Development LLC.; Lumosity; Lundbeck; Merck & Co., Inc.; Meso Scale Diagnostics, LLC.; NeuroRx Research; Neurotrack Technologies; Novartis Pharmaceuticals Corporation; Pfizer Inc.; Piramal Imaging; Servier; Takeda Pharmaceutical Company; and Transition Therapeutics. The Canadian Institutes of Health Research is providing funds to support ADNI clinical sites in Canada. Private sector contributions are facilitated by the Foundation for the National Institutes of Health (www.fnih.org). The grantee organization is the Northern California Institute for Research and Education, and the study is coordinated by the Alzheimer's Therapeutic Research Institute at the University of Southern California. ADNI data are disseminated by the Laboratory for Neuro Imaging at the University of Southern California.

Funding

This work was supported by the National Institutes of Health AG073259, AG049089, AG059065, AG073927, AG068399, and Foundation of Hope.

Conflict of Interest

All other authors have no conflict of interest to report.

Data Availability

This work is mainly a secondary data analysis on ADNI data, where all the imaging data and phenotyping data are available at <https://adni.loni.usc.edu/>

References

- Altmann, A., Tian, L., Henderson, V.W., Greicius, M.D., 2014. Sex modifies the APOE-related risk of developing Alzheimer disease. *Ann Neurol* 75, 563-573.
- Anchisi, D., Borroni, B., Franceschi, M., Kerrouche, N., Kalbe, E., Beuthien-Beumann, B., Cappa, S., Lenz, O., Ludecke, S., Marcone, A., Mielke, R., Ortelli, P., Padovani, A., Pelati, O., Pupi, A., Scarpini, E., Weisenbach, S., Herholz, K., Salmon, E., Holthoff, V., Sorbi, S., Fazio, F., Perani, D., 2005. Heterogeneity of brain glucose metabolism in mild cognitive impairment and clinical progression to Alzheimer disease. *Arch Neurol* 62.
- Andrew, M.K., Tierney, M.C., 2018. The puzzle of sex, gender and Alzheimer's disease: Why are women more often affected than men? *Women's Health* 14, 1745506518817995.
- Arevalo-Rodriguez, I., Smailagic, N., Roqué, I.F.M., Ciapponi, A., Sanchez-Perez, E., Giannakou, A., Pedraza, O.L., Bonfill Cosp, X., Cullum, S., 2015. Mini-Mental State Examination (MMSE) for the detection of Alzheimer's disease and other dementias in people with mild cognitive impairment (MCI). *Cochrane Database Syst Rev* 2015, Cd010783.
- Arnold, T.B., Tibshirani, R.J., 2016. Efficient Implementations of the Generalized Lasso Dual Path Algorithm. *Journal of Computational and Graphical Statistics* 25, 1-27.
- Barnes, L.L., Wilson, R.S., Bienias, J.L., Schneider, J.A., Evans, D.A., Bennett, D.A., 2005. Sex Differences in the Clinical Manifestations of Alzheimer Disease Pathology. *Archives of General Psychiatry* 62, 685-691.
- Campbell, M.R., Ashrafzadeh-Kian, S., Petersen, R.C., Mielke, M.M., Syrjanen, J.A., van Harten, A.C., Lowe, V.J., Jack, C.R., Jr., Bornhorst, J.A., Algeciras-Schimmin, A., 2021. P-tau/A β 42 and A β 42/40 ratios in CSF are equally predictive of amyloid PET status. *Alzheimers Dement (Amst)* 13, e12190.
- Chan, N.H., Yau, C.Y., Zhang, R.-M., 2014. Group LASSO for Structural Break Time Series. *Journal of the American Statistical Association* 109, 590-599.
- Chen, P., Yao, H., Tijms, B.M., Wang, P., Wang, D., Song, C., Yang, H., Zhang, Z., Zhao, K., Qu, Y., Kang, X., Du, K., Fan, L., Han, T., Yu, C., Zhang, X., Jiang, T., Zhou, Y., Lu, J., Han, Y., Liu, B., Zhou, B., Liu, Y., Four Distinct Subtypes of Alzheimer's Disease Based on Resting-State Connectivity Biomarkers. *Biol Psychiatry*.
- Clark, C.M., Sheppard, L., Fillenbaum, G.G., Galasko, D., Morris, J.C., Koss, E., Mohs, R., Heyman, A., Investigators, a.t.C., 1999. Variability in Annual Mini-Mental State Examination Score in Patients With Probable Alzheimer Disease: A Clinical Perspective of Data From the Consortium to Establish a Registry for Alzheimer's Disease. *Archives of Neurology* 56, 857-862.
- Davis, E.J., Solsberg, C.W., White, C.C., Miñones-Moyano, E., Sirota, M., Chibnik, L., Bennett, D.A., De Jager, P.L., Yokoyama, J.S., Dubal, D.B., 2021. Sex-Specific Association of the X Chromosome With Cognitive Change and Tau Pathology in Aging and Alzheimer Disease. *JAMA Neurology* 78, 1249-1254.
- Destrieux, C., Fischl, B., Dale, A., Halgren, E., 2010. Automatic parcellation of human cortical gyri and sulci using standard anatomical nomenclature. *Neuroimage* 53, 1-15.
- Dong, A., Honnorat, N., Gaonkar, B., Davatzikos, C., 2016. CHIMERA: Clustering of Heterogeneous Disease Effects via Distribution Matching of Imaging Patterns. *IEEE Trans Med Imaging* 35, 612-621.

- Dong, A., Toledo, J.B., Honnorat, N., Doshi, J., Varol, E., Sotiras, A., Wolk, D., Trojanowski, J.Q., Davatzikos, C., 2017a. Heterogeneity of neuroanatomical patterns in prodromal Alzheimer's disease: links to cognition, progression and biomarkers. *Brain* 140, 735-747.
- Dong, A., Toledo, J.B., Honnorat, N., Doshi, J., Varol, E., Sotiras, A., Wolk, D., Trojanowski, J.Q., Davatzikos, C., 2017b. Heterogeneity of neuroanatomical patterns in prodromal Alzheimer's disease: links to cognition, progression and biomarkers. *Brain* 140, 735-747.
- Dunn, A.R., O'Connell, K.M.S., Kaczorowski, C.C., 2019. Gene-by-environment interactions in Alzheimer's disease and Parkinson's disease. *Neuroscience & Biobehavioral Reviews* 103, 73-80.
- Eid, A., Mhatre, I., Richardson, J.R., 2019. Gene-environment interactions in Alzheimer's disease: A potential path to precision medicine. *Pharmacology & Therapeutics* 199, 173-187.
- Elbaz, A., Dufouil, C., Alpérovitch, A., 2007. Interaction between genes and environment in neurodegenerative diseases. *C R Biol* 330, 318-328.
- Fawns-Ritchie, C., Deary, I.J., 2020. Reliability and validity of the UK Biobank cognitive tests. *PLoS One* 15, e0231627.
- Firth, N.C., Primativo, S., Brotherhood, E., Young, A.L., Yong, K.X.X., Crutch, S.J., Alexander, D.C., Oxtoby, N.P., 2020. Sequences of cognitive decline in typical Alzheimer's disease and posterior cortical atrophy estimated using a novel event-based model of disease progression. *Alzheimers Dement* 16, 965-973.
- Fischl, B., 2012. FreeSurfer. *Neuroimage* 62, 774-781.
- Fryzlewicz, P., 2014. Wild binary segmentation for multiple change-point detection. *The Annals of Statistics* 42, 2243-2281.
- Gibbons, L.E., Carle, A.C., Mackin, R.S., Harvey, D., Mukherjee, S., Insel, P., Curtis, S.M., Mungas, D., Crane, P.K., 2012. A composite score for executive functioning, validated in Alzheimer's Disease Neuroimaging Initiative (ADNI) participants with baseline mild cognitive impairment. *Brain Imaging Behav* 6, 517-527.
- Hampel, H., Cummings, J., Blennow, K., Gao, P., Jack, C.R., Jr., Vergallo, A., 2021. Developing the ATX(N) classification for use across the Alzheimer disease continuum. *Nat Rev Neurol* 17, 580-589.
- Hwang, J., Kim, C.M., Jeon, S., Lee, J.M., Hong, Y.J., Roh, J.H., Lee, J.H., Koh, J.Y., Na, D.L., 2016. Prediction of Alzheimer's disease pathophysiology based on cortical thickness patterns. *Alzheimers Dement (Amst)* 2, 58-67.
- Iqbal, K., Grundke-Iqbali, I., 2010. Alzheimer's disease, a multifactorial disorder seeking multitherapies. *Alzheimers Dement* 6, 420-424.
- Jack, C.R., Bennett, D.A., Blennow, K., Carrillo, M.C., Dunn, B., Haeberlein, S.B., Holtzman, D.M., Jagust, W., Jessen, F., Karlawish, J., Liu, E., Molinuevo, J.L., Montine, T., Phelps, C., Rankin, K.P., Rowe, C.C., Scheltens, P., Siemers, E., Snyder, H.M., Sperling, R., Elliott, C., Masliah, E., Ryan, L., Silverberg, N., 2018. NIA-AA Research Framework: Toward a biological definition of Alzheimer's disease. *Alzheimer's & Dementia* 14, 535-562.
- Jack, C.R., Jr., Bennett, D.A., Blennow, K., Carrillo, M.C., Feldman, H.H., Frisoni, G.B., Hampel, H., Jagust, W.J., Johnson, K.A., Knopman, D.S., Petersen, R.C., Scheltens, P., Sperling, R.A., Dubois, B., 2016. A/T/N: An unbiased descriptive classification scheme for Alzheimer disease biomarkers. *Neurology* 87, 539-547.
- Jack, C.R., Knopman, D.S., Jagust, W.J., Petersen, R.C., Weiner, M.W., Aisen, P.S., Shaw, L.M., Vemuri, P., Wiste, H.J., Weigand, S.D., Lesnick, T.G., Pankratz, V.S., Donohue, M.C., Trojanowski, J.Q., 2013. Tracking pathophysiological processes in Alzheimer's disease: an updated hypothetical model of dynamic biomarkers. *The Lancet Neurology* 12, 207-216.
- Jin, B., Shi, X., Wu, Y., 2013. A novel and fast methodology for simultaneous multiple structural break estimation and variable selection for nonstationary time series models. *Statistics and Computing* 23, 221-231.
- Lam, B., Masellis, M., Freedman, M., Stuss, D., Black, S., 2013. Clinical, imaging, and pathological heterogeneity of the Alzheimer's disease syndrome. *Alzheimers Res Ther* 5.
- Lee, S., Seo, M.H., Shin, Y., 2016. The Lasso for High Dimensional Regression with a Possible Change Point. *Journal of the Royal Statistical Society Series B: Statistical Methodology* 78, 193-210.

- Liu, B., Zhang, X., Liu, Y., 2021. Simultaneous Change Point Inference and Structure Recovery for High Dimensional Gaussian Graphical Models. *Journal of machine Learning Research* 22, 1-62.
- Liu, B., Zhang, X., Liu, Y., 2022. High dimensional change point inference: Recent developments and extensions. *Journal of Multivariate Analysis* 188, 104833.
- Liu, B., Zhou, C., Zhang, X., Liu, Y., 2020. A unified data-adaptive framework for high dimensional change point detection. *Journal of the Royal Statistical Society Series B* 82, 933-963.
- Ma, H., Liu, Y., Wu, G., 2022. Elucidating Multi-Stage Progression of Neuro-degeneration Process in Alzheimer's Disease. *Alzheimer's & Dementia* 18.
- Maidstone, R., Hocking, T., Rigaill, G., Fearnhead, P., 2017. On optimal multiple changepoint algorithms for large data. *Statistics and Computing* 27, 519-533.
- Medaglia, J.D., Pasqualetti, F., Hamilton, R.H., Thompson-Schill, S.L., Bassett, D.S., 2017. Brain and cognitive reserve: Translation via network control theory. *Neuroscience & Biobehavioral Reviews* 75, 53-64.
- Mu, W., Davis, E.S., Lee, S., Dozmanov, M.G., Phanstiel, D.H., Love, M.I., 2023. bootRanges: flexible generation of null sets of genomic ranges for hypothesis testing. *Bioinformatics* 39.
- Mu, W., Sarkar, H., Srivastava, A., Choi, K., Patro, R., Love, M.I., 2022. Airport: interpretable statistical models for analyzing allelic imbalance in single-cell datasets. *Bioinformatics* 38, 2773-2780.
- Noh, Y., Jeon, S., Lee, J.M., Seo, S.W., Kim, G.H., Cho, H., Ye, B.S., Yoon, C.W., Kim, H.J., Chin, J., Park, K.H., Heilman, K.M., Na, D.L., 2014. Anatomical heterogeneity of Alzheimer disease: based on cortical thickness on MRIs. *Neurology* 83, 1936-1944.
- Organization, W.H., 2012. *Dementia: A Public Health Priority*. World Health Organization.
- Reed, B.R., Mungas, D., Farias, S.T., Harvey, D., Beckett, L., Widaman, K., Hinton, L., DeCarli, C., 2010. Measuring cognitive reserve based on the decomposition of episodic memory variance. *Brain* 133, 2196-2209.
- Sacktor, N., Soldan, A., Grega, M., Farrington, L., Cai, Q., Wang, M.C., Gottesman, R.F., Turner, R.S., Albert, M., 2017. The BIOCARD Index: A Summary Measure to Predict Onset of Mild Cognitive Impairment. *Alzheimer Dis Assoc Disord* 31, 114-119.
- Stern, Y., 2002. What is cognitive reserve? Theory and research application of the reserve concept. *Journal of the International Neuropsychological Society* 8, 448-460.
- Stern, Y., 2006. Cognitive Reserve and Alzheimer Disease. *Alzheimer Disease & Associated Disorders* 20, 112-117.
- Stern, Y., 2012. Cognitive reserve in ageing and Alzheimer's disease. *Lancet Neurol* 11, 1006-1012.
- Stern, Y., 2017. An approach to studying the neural correlates of reserve. *Brain Imaging and Behavior* 11, 410-416.
- Stern, Y., Arenaza-Urquijo, E.M., Bartrés-Faz, D., Belleville, S., Cantillon, M., Chetelat, G., Ewers, M., Franzmeier, N., Kempermann, G., Kremen, W.S., Okonkwo, O., Scarmeas, N., Soldan, A., Udeh-Momoh, C., Valenzuela, M., Vemuri, P., Vuoksimaa, E., and the Reserve, R., Definitions, P.F.P.E., Workgroup, C.F., 2020. Whitepaper: Defining and investigating cognitive reserve, brain reserve, and brain maintenance. *Alzheimer's & Dementia* 16, 1305-1311.
- Tatsuoka, C., Tseng, H., Jaeger, J., Varadi, F., Smith, M.A., Yamada, T., Smyth, K.A., Lerner, A.J., 2013. Modeling the heterogeneity in risk of progression to Alzheimer's disease across cognitive profiles in mild cognitive impairment. *Alzheimers Res Ther* 5.
- Tibshirani, R., 1996. Regression Shrinkage and Selection via the Lasso. *Journal of Royal Statistical Society, Series B (Methodological)* 58, 267-288.
- van de Geer, S., Bühlmann, P., Ritov, Y.a., Dezeure, R., 2014. ON ASYMPTOTICALLY OPTIMAL CONFIDENCE REGIONS AND TESTS FOR HIGH-DIMENSIONAL MODELS. *The Annals of Statistics* 42, 1166-1202.
- van Loenhoud, A.C., van der Flier, W.M., Wink, A.M., Dicks, E., Groot, C., Twisk, J., Barkhof, F., Scheltens, P., Ossenkoppele, R., 2019. Cognitive reserve and clinical progression in Alzheimer disease. *Neurology* 93, e334.

- van Loenhoud, A.C., Wink, A.M., Groot, C., Verfaillie, S.C.J., Twisk, J., Barkhof, F., van Berckel, B., Scheltens, P., van der Flier, W.M., Ossenkoppele, R., 2017. A neuroimaging approach to capture cognitive reserve: Application to Alzheimer's disease. *Hum Brain Mapp* 38, 4703-4715.
- Vogel, J.W., Young, A.L., Oxtoby, N.P., Smith, R., Ossenkoppele, R., Strandberg, O.T., La Joie, R., Aksman, L.M., Grothe, M.J., Iturria-Medina, Y., Weiner, M., Aisen, P., Petersen, R., Jack, C.R., Jagust, W., Trojanowski, J.Q., Toga, A.W., Beckett, L., Green, R.C., Saykin, A.J., Morris, J., Shaw, L.M., Liu, E., Montine, T., Thomas, R.G., Donohue, M., Walter, S., Gessert, D., Sather, T., Jiminez, G., Harvey, D., Bernstein, M., Fox, N., Thompson, P., Schuff, N., DeCarli, C., Borowski, B., Gunter, J., Senjem, M., Vemuri, P., Jones, D., Kantarci, K., Ward, C., Koeppe, R.A., Foster, N., Reiman, E.M., Chen, K., Mathis, C., Landau, S., Cairns, N.J., Householder, E., Reinwald, L.T., Lee, V., Korecka, M., Figurski, M., Crawford, K., Neu, S., Foroud, T.M., Potkin, S., Shen, L., Kelley, F., Kim, S., Nho, K., Kachaturian, Z., Frank, R., Snyder, P.J., Molchan, S., Kaye, J., Quinn, J., Lind, B., Carter, R., Dolen, S., Schneider, L.S., Pawluczyk, S., Beccera, M., Teodoro, L., Spann, B.M., Brewer, J., Vanderswag, H., Fleisher, A., Heidebrink, J.L., Lord, J.L., Mason, S.S., Albers, C.S., Knopman, D., Johnson, K., Doody, R.S., Meyer, J.V., Chowdhury, M., Rountree, S., Dang, M., Stern, Y., Honig, L.S., Bell, K.L., Ances, B., Morris, J.C., Carroll, M., Leon, S., Mintun, M.A., Schneider, S., Oliver, A., Griffith, R., Clark, D., Geldmacher, D., Brockington, J., Roberson, E., Grossman, H., Mitsis, E., deToledo-Morrell, L., Shah, R.C., Duara, R., Varon, D., Greig, M.T., Roberts, P., Albert, M., Onyike, C., D'Agostino, D., Kielb, S., Galvin, J.E., Pogorelec, D.M., Cerbone, B., Michel, C.A., Rusinek, H., de Leon, M.J., Glodzik, L., De Santi, S., Doraiswamy, P.M., Petrella, J.R., Wong, T.Z., Arnold, S.E., Karlawish, J.H., Wolk, D., Smith, C.D., Jicha, G., Hardy, P., Sinha, P., Oates, E., Conrad, G., Lopez, O.L., Oakley, M., Simpson, D.M., Porsteinsson, A.P., Goldstein, B.S., Martin, K., Makino, K.M., Ismail, M.S., Brand, C., Mulnard, R.A., Thai, G., McAdams Ortiz, C., Womack, K., Mathews, D., Quiceno, M., Arrastia, R.D., King, R., Weiner, M., Cook, K.M., DeVos, M., Levey, A.I., Lah, J.J., Cellar, J.S., Burns, J.M., Anderson, H.S., Swerdlow, R.H., Apostolova, L., Tingus, K., Woo, E., Silverman, D.H.S., Lu, P.H., Bartzokis, G., Radford, N.R.G., Parfitt, F., Kendall, T., Johnson, H., Farlow, M.R., Hake, A.M., Matthews, B.R., Herring, S., Hunt, C., van Dyck, C.H., Carson, R.E., MacAvoy, M.G., Chertkow, H., Bergman, H., Hosein, C., Black, S., Stefanovic, B., Caldwell, C., Hsiung, G.Y.R., Feldman, H., Mudge, B., Past, M.A., Kertesz, A., Rogers, J., Trost, D., Bernick, C., Munic, D., Kerwin, D., Mesulam, M.M., Lipowski, K., Wu, C.K., Johnson, N., Sadowsky, C., Martinez, W., Villena, T., Turner, R.S., Johnson, K., Reynolds, B., Sperling, R.A., Johnson, K.A., Marshall, G., Frey, M., Yesavage, J., Taylor, J.L., Lane, B., Rosen, A., Tinklenberg, J., Sabbagh, M.N., Belden, C.M., Jacobson, S.A., Sirrel, S.A., Kowall, N., Killiany, R., Budson, A.E., Norbash, A., Johnson, P.L., Obisesan, T.O., Wolday, S., Allard, J., Lerner, A., Ogorcki, P., Hudson, L., Fletcher, E., Carmichael, O., Olichney, J., DeCarli, C., Kittur, S., Borrie, M., Lee, T.Y., Bartha, R., Johnson, S., Asthana, S., Carlsson, C.M., Potkin, S.G., Preda, A., Nguyen, D., Tariot, P., Reeder, S., Bates, V., Capote, H., Rainka, M., Scharre, D.W., Kataki, M., Adeli, A., Zimmerman, E.A., Celmins, D., Brown, A.D., Pearson, G.D., Blank, K., Anderson, K., Santulli, R.B., Kitzmiller, T.J., Schwartz, E.S., Sink, K.M., Williamson, J.D., Garg, P., Watkins, F., Ott, B.R., Querfurth, H., Tremont, G., Salloway, S., Malloy, P., Correia, S., Rosen, H.J., Miller, B.L., Mintzer, J., Spicer, K., Bachman, D., Finger, E., Pasternak, S., Rachinsky, I., Drost, D., Pomara, N., Hernando, R., Sarrael, A., Schultz, S.K., Ponto, L.L.B., Shim, H., Smith, K.E., Relkin, N., Chaing, G., Raudin, L., Smith, A., Fargher, K., Raj, B.A., Pontecorvo, M.J., Devous, M.D., Rabinovici, G.D., Alexander, D.C., the Alzheimer's Disease Neuroimaging, I., 2021. Four distinct trajectories of tau deposition identified in Alzheimer's disease. *Nature Medicine* 27, 871-881.
- Whitwell, J.L., Graff-Radford, J., Tosakulwong, N., Weigand, S.D., Machulda, M., Senjem, M.L., Schwarz, C.G., Spychalla, A.J., Jones, D.T., Drubach, D.A., Knopman, D.S., Boeve, B.F., Ertekin-Taner, N., Petersen, R.C., Lowe, V.J., Jack, C.R., Jr., Josephs, K.A., 2018. [(18) F]AV-1451 clustering of entorhinal and cortical uptake in Alzheimer's disease. *Ann Neurol* 83, 248-257.
- Wolk, D.A., Price, J.C., Saxton, J.A., Snitz, B.E., James, J.A., Lopez, O.L., Aizenstein, H.J., Cohen, A.D., Weissfeld, L.A., Mathis, C.A., Klunk, W.E., De-Kosky, S.T., 2009. Amyloid imaging in mild cognitive impairment subtypes. *Ann Neurol* 65,

Young, A.L., Marinescu, R.V., Oxtoby, N.P., Bocchetta, M., Yong, K., Firth, N.C., Cash, D.M., Thomas, D.L., Dick, K.M., Cardoso, J., van Swieten, J., Borroni, B., Galimberti, D., Masellis, M., Tartaglia, M.C., Rowe, J.B., Graff, C., Tagliavini, F., Frisoni, G.B., Laforce, R., Finger, E., de Mendonça, A., Sorbi, S., Warren, J.D., Crutch, S., Fox, N.C., Ourselin, S., Schott, J.M., Rohrer, J.D., Alexander, D.C., Andersson, C., Archetti, S., Arighi, A., Benussi, L., Binetti, G., Black, S., Cosseddu, M., Fallström, M., Ferreira, C., Fenoglio, C., Freedman, M., Fumagalli, G.G., Gazzina, S., Ghidoni, R., Grisolí, M., Jelic, V., Jiskoot, L., Keren, R., Lombardi, G., Maruta, C., Meeter, L., Mead, S., van Minkelen, R., Naemias, B., Öijerstedt, L., Padovani, A., Panman, J., Pievani, M., Polito, C., Premi, E., Priomì, S., Rademakers, R., Redaelli, V., Rogaea, E., Rossi, G., Rossor, M., Scarpini, E., Tang-Wai, D., Thonberg, H., Tiraboschi, P., Verdelho, A., Weiner, M.W., Aisen, P., Petersen, R., Jack, C.R., Jagust, W., Trojanowski, J.Q., Toga, A.W., Beckett, L., Green, R.C., Saykin, A.J., Morris, J., Shaw, L.M., Khachaturian, Z., Sorensen, G., Kuller, L., Raichle, M., Paul, S., Davies, P., Fillit, H., Hefti, F., Holtzman, D., Mesulam, M.M., Potter, W., Snyder, P., Schwartz, A., Montine, T., Thomas, R.G., Donohue, M., Walter, S., Gessert, D., Sather, T., Jiminez, G., Harvey, D., Bernstein, M., Thompson, P., Schuff, N., Borowski, B., Gunter, J., Senjem, M., Vemuri, P., Jones, D., Kantarci, K., Ward, C., Koeppe, R.A., Foster, N., Reiman, E.M., Chen, K., Mathis, C., Landau, S., Cairns, N.J., Householder, E., Taylor-Reinwald, L., Lee, V., Korecka, M., Figurski, M., Crawford, K., Neu, S., Foroud, T.M., Potkin, S., Shen, L., Faber, K., Kim, S., Nho, K., Thal, L., Buckholtz, N., Albert, M., Frank, R., Hsiao, J., Kaye, J., Quinn, J., Lind, B., Carter, R., Dolen, S., Schneider, L.S., Pawluczyk, S., Beccera, M., Teodoro, L., Spann, B.M., Brewer, J., Vanderswag, H., Fleisher, A., Heidebrink, J.L., Lord, J.L., Mason, S.S., Albers, C.S., Knopman, D., Johnson, K., Doody, R.S., Villanueva-Meyer, J., Chowdhury, M., Rountree, S., Dang, M., Stern, Y., Honig, L.S., Bell, K.L., Ances, B., Carroll, M., Leon, S., Mintun, M.A., Schneider, S., Oliver, A., Marson, D., Griffith, R., Clark, D., Geldmacher, D., Brockington, J., Roberson, E., Grossman, H., Mitsis, E., de Toledo-Morrell, L., Shah, R.C., Duara, R., Varon, D., Greig, M.T., Roberts, P., Albert, M., Onyike, C., D'Agostino, D., Kielb, S., Galvin, J.E., Cerbone, B., Michel, C.A., Rusinek, H., de Leon, M.J., Glodzik, L., De Santi, S., Doraiswamy, P.M., Petrella, J.R., Wong, T.Z., Arnold, S.E., Karlawish, J.H., Wolk, D., Smith, C.D., Jicha, G., Hardy, P., Sinha, P., Oates, E., Conrad, G., Lopez, O.L., Oakley, M., Simpson, D.M., Porsteinsson, A.P., Goldstein, B.S., Martin, K., Makino, K.M., Ismail, M.S., Brand, C., Mulnard, R.A., Thai, G., Mc-Adams-Ortiz, C., Womack, K., Mathews, D., Quiceno, M., Diaz-Arrastia, R., King, R., Weiner, M., Martin-Cook, K., DeVous, M., Levey, A.I., Lah, J.J., Cellar, J.S., Burns, J.M., Anderson, H.S., Swerdlow, R.H., Apostolova, L., Tingus, K., Woo, E., Silverman, D.H., Lu, P.H., Bartzokis, G., Graff-Radford, N.R., Parfitt, F., Kendall, T., Johnson, H., Farlow, M.R., Hake, A.M., Matthews, B.R., Herring, S., Hunt, C., van Dyck, C.H., Carson, R.E., MacAvoy, M.G., Chertkow, H., Bergman, H., Hosein, C., Stefanovic, B., Caldwell, C., Hsiung, G.-Y.R., Feldman, H., Mudge, B., Assaly, M., Kertesz, A., Rogers, J., Bernick, C., Munic, D., Kerwin, D., Mesulam, M.-M., Lipowski, K., Wu, C.-K., Johnson, N., Sadowsky, C., Martinez, W., Villena, T., Turner, R.S., Johnson, K., Reynolds, B., Sperling, R.A., Johnson, K.A., Marshall, G., Frey, M., Lane, B., Rosen, A., Tinklenberg, J., Sabbagh, M.N., Belden, C.M., Jacobson, S.A., Sirrel, S.A., Kowall, N., Killiany, R., Budson, A.E., Norbash, A., Johnson, P.L., Allard, J., Lerner, A., Ogrocki, P., Hudson, L., Fletcher, E., The Genetic, F.T.D.I., The Alzheimer's Disease Neuroimaging, I., 2018. Uncovering the heterogeneity and temporal complexity of neurodegenerative diseases with Subtype and Stage Inference. Nat Commun 9, 4273. Zhang, B., Geng, J., Lai, L., 2015. Change-point estimation in high dimensional linear regression models via sparse group Lasso. 53rd Annual Allerton Conference on Communication, Control, and Computing (Allerton). IEEE, 815-821.

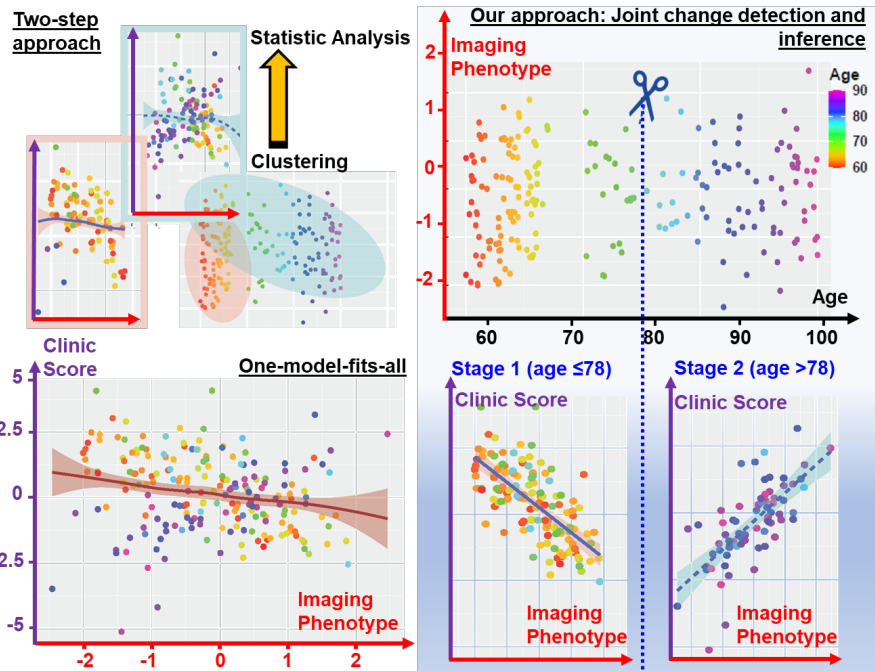


Fig. 1. Current two-step approach (top-left) vs our joint change detection and statistical inference (bottom-right). The distribution of simulated data is shown in top-right, where applying a global regression model on the whole data (bottom-left) does not have the statistical power to model the relationship between imaging phenotype and clinical outcomes. Since current two-step approaches apply clustering and statistical analysis separately, the clustering result might be sub-optimal for statistical inference. Our method disentangles the heterogeneity of temporal behavior (i.e., the relationship between imaging phenotype and clinical outcome) and thus yield significantly higher statistical power in understanding the factors behind the clinical outcomes.

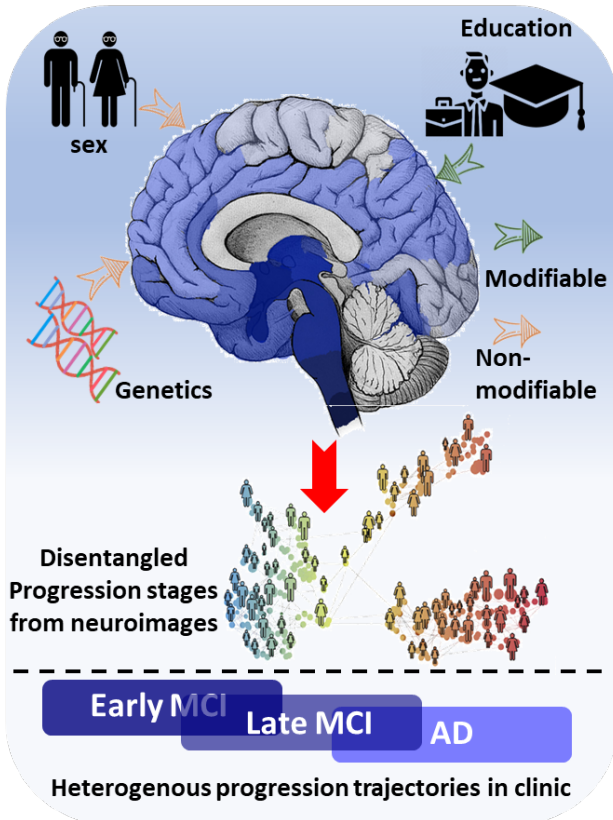


Fig. 2. Our statistical model identifies change points, sorted by age, by examining the latent piecewise linear relationship between regional AD biomarkers and clinical outcomes. Using the results from temporal stratification, we are able to explore how biological sex and education level dynamically contribute to modifying the impact of *APOE4* on cognitive decline across multiple stages of AD progression.

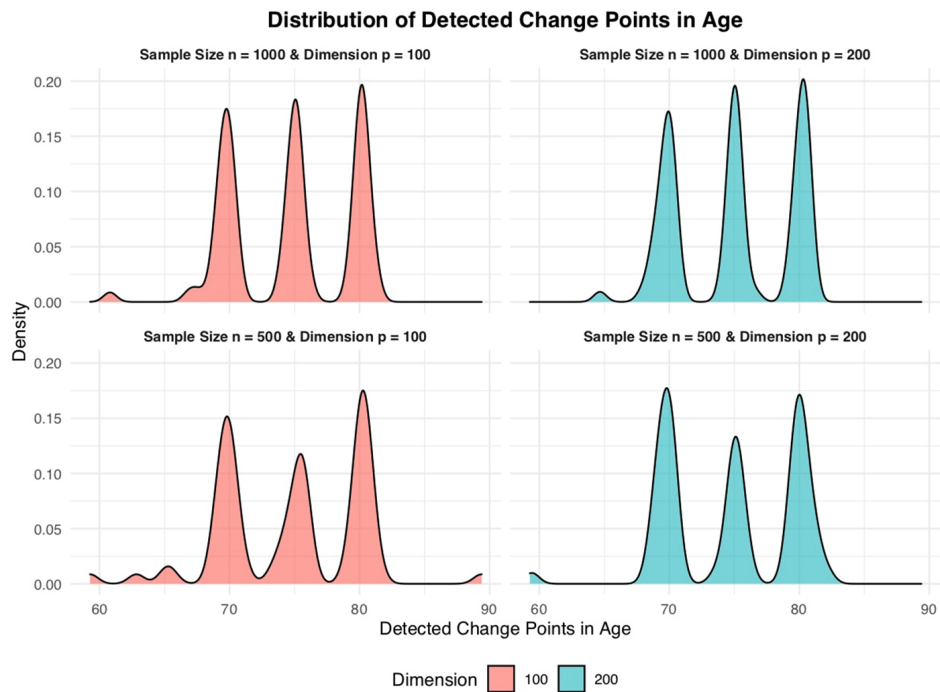


Fig. 3. Density plots of detected change points for multiple change point case.

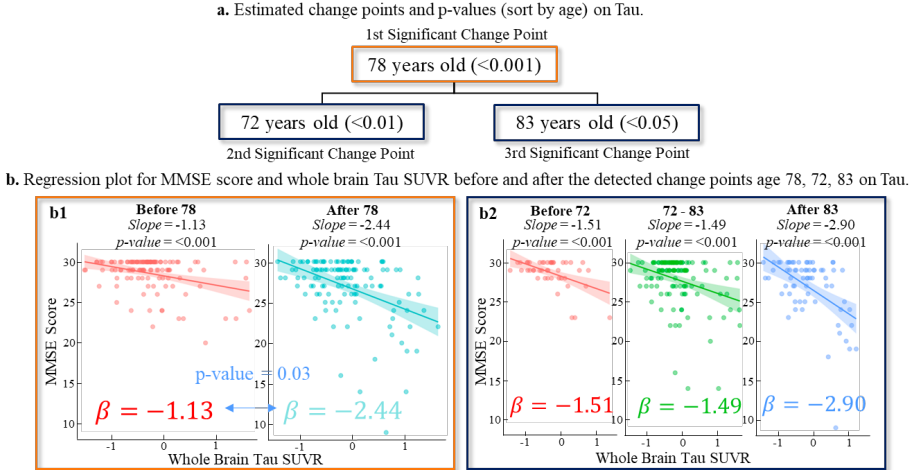
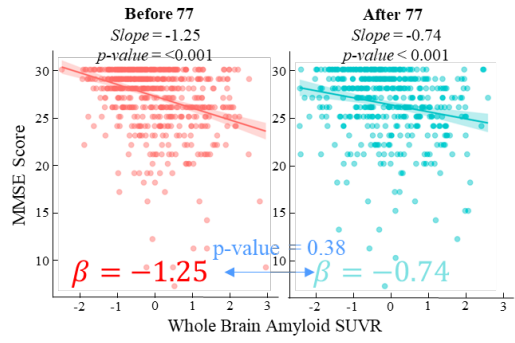


Fig. 4. The change point detection results on T-biomarker. (a) There are three significant change points occurring at the ages of 72, 78, and 83, where the temporal patterns of T~MMSE relationship manifest significant difference before and after changing point. (b) The fitted line of T~MMSE relationships before and after change points.

a. Regression plot for MMSE score and whole brain Amyloid SUVR before and after the detected change point age 77 ($p\text{-value} = 0.40$) on Amyloid.



b. Mean Square Error of two regression models.

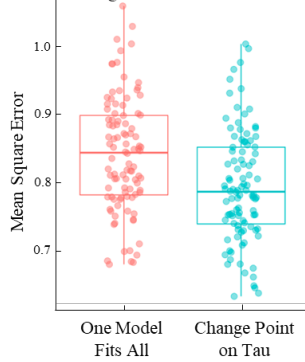
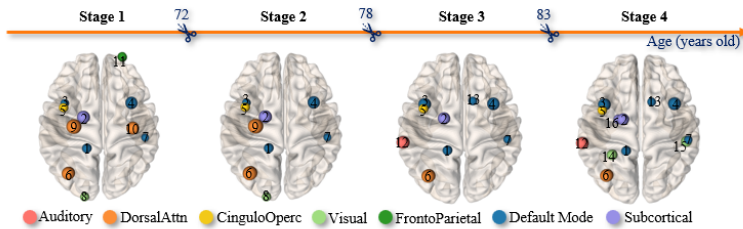


Fig. 5. The change point detection results on A biomarker. (a) We have not found significant change point in A~MMSE relationship as the linear model before the age of 77 (in red) does not show significant difference with comparison to that after the age of 77 (in green). (b) Reduced fitting error of T~MMSE relationship by piecewise line fitting (in green) for each progression stage, compared to global linear model (in red).

a. The coefficient of each stage on Tau in brain distribution.**b.** The summary of brain regions.

| | Stage 1 | Stage 2 | Stage 3 | Stage 4 | | Stage 1 | Stage 2 | Stage 3 | Stage 4 |
|--|---------|---------|---------|---------|---|---------|---------|---------|---------|
| #1 Posterior-ventral part of the cingulate gyrus | ✓ | ✓ | ✓ | ✓ | #9 Left superior part of the precentral sulcus | ✓ | ✓ | | |
| #2 Left hemisphere globus pallidus | ✓ | ✓ | ✓ | ✓ | #10 Right superior part of the precentral sulcus | ✓ | | | |
| #3 Left temporal pole | ✓ | ✓ | ✓ | ✓ | #11 Transverse frontopolar gyri and sulci | ✓ | | | |
| #4 Right temporal pole | ✓ | ✓ | ✓ | ✓ | #12 Planum temporale of the superior temporal gyrus | ✓ | ✓ | | |
| #5 Superior segment of the circular sulcus of the insula | ✓ | ✓ | ✓ | ✓ | #13 Subcallosal gyrus | ✓ | ✓ | | |
| #6 Intraparietal sulcus and transverse parietal sulci | ✓ | ✓ | ✓ | ✓ | #14 Lateral occipito-temporal gyrus | ✓ | | | |
| #7 Inferior temporal sulcus | ✓ | ✓ | ✓ | ✓ | #15 Inferior temporal gyrus | ✓ | | | |
| #8 Superior occipital gyrus | ✓ | ✓ | | | #16 Left hemisphere hippocampus | ✓ | | | |

Fig. 6. The change point detection results on T biomarker. (a) The brain regions on which T-biomarkers have top-ranked contributions to the transitions. (b) The summary of brain regions that have the most significant impact on the occurrence of changing points.

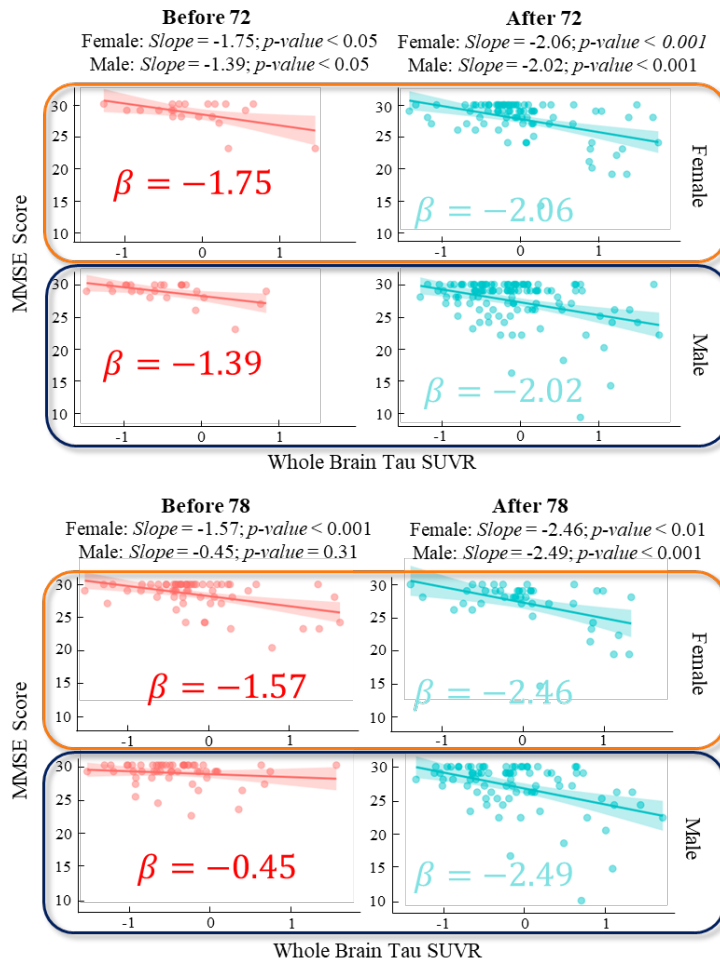


Fig. 7. Regression plot for MMSE score and whole brain Tau SUVR before and after the detected change points age 72 (top) and 78 (bottom) on Tau and stratified by sex.

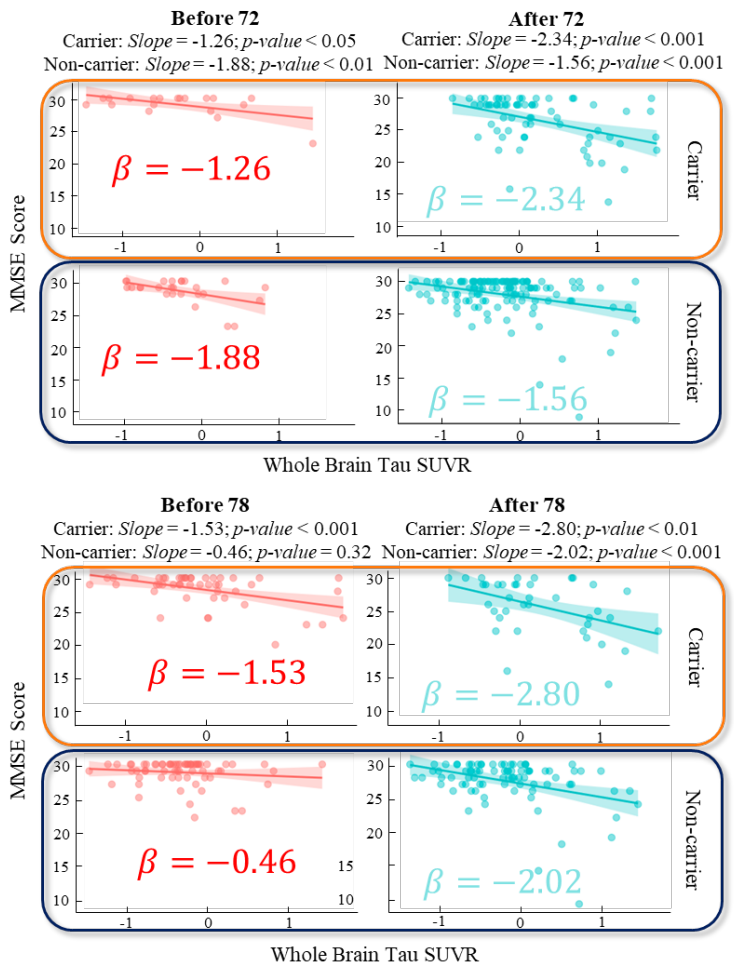


Fig. 8. Regression plot for MMSE score and whole brain Tau SUVR before and after the detected change points age 72 (top) and 78 (bottom) on Tau and stratified by *APOE4* carrier and non-carrier.

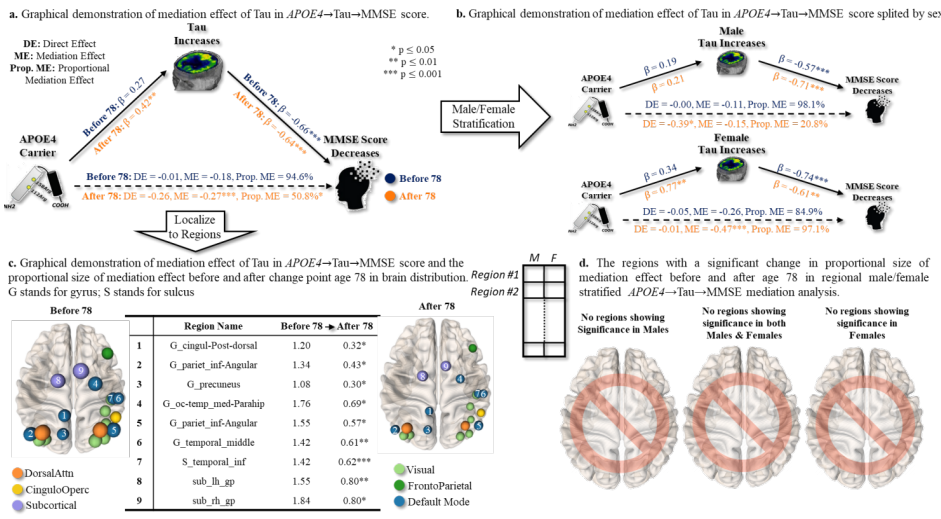


Fig. 9. Sex-dependent effect of *APOE4* on cognitive decline, possibly mediated by T-biomarker in the *APOE4*→Tau→MMSE pathway. (a) We first examine the direct effect (*APOE4*→MMSE) and the corresponding indirect effect mediated by whole-brain T biomarkers before and after particular change point. (b) Then, we stratify the same mediation analysis to males and females separately. (c) Furthermore, we conduct the same mediation analysis (males and females together) at each brain region. We display the mediation effect before and after change point (right), where the node size indicates the proportion of mediation effect size. (d) Finally, we investigate whether the regional *APOE4*→Tau→MMSE pathways manifest significant changes in the proportion of mediation effect (by T-biomarker) before and after age 78 in the male/female stratified mediation analysis.

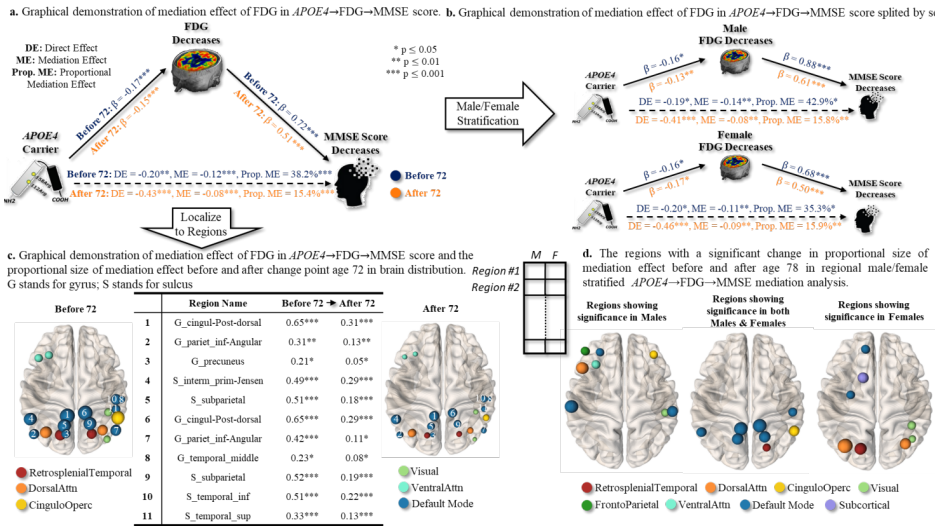
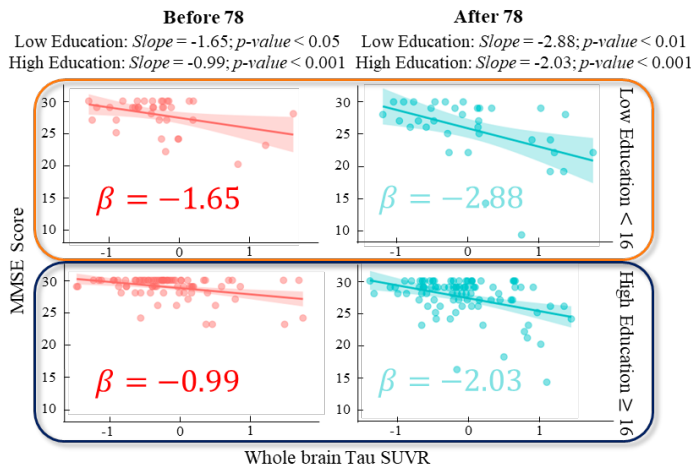


Fig. 10. Sex-dependent effect of $APOE4$ on cognitive decline, possibly mediated by [N]-biomarker in the $APOE4 \rightarrow$ FDG \rightarrow MMSE pathway. (a) We first examine the direct effect ($APOE4 \rightarrow$ MMSE) and the corresponding indirect effect mediated by whole-brain [N] biomarkers before and after particular change point. (b) Then, we stratify the same mediation analysis to males and females separately. (c) Furthermore, we conduct the same mediation analysis (males and females together) at each brain region. We display the mediation effect before and after change point (right), where the node size indicates the proportion of mediation effect size. (d) Finally, we investigate whether the regional $APOE4 \rightarrow$ FDG \rightarrow MMSE pathways manifest significant changes in the proportion of mediation effect (by [N]-biomarker) before and after age 72 in the male/female stratified mediation analysis.

a. Regression plot for MMSE score and whole brain Tau burden before and after the detected change points age 78 for low and high-education groups.



b. Graphical demonstration of mediation effect of T-biomarker in *APOE4*→Tau→MMSE score stratified by low and high-education level.

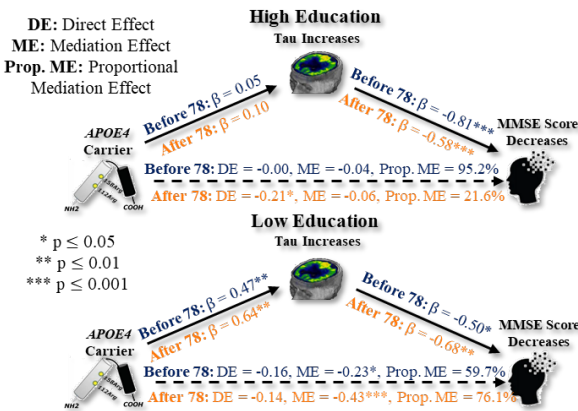
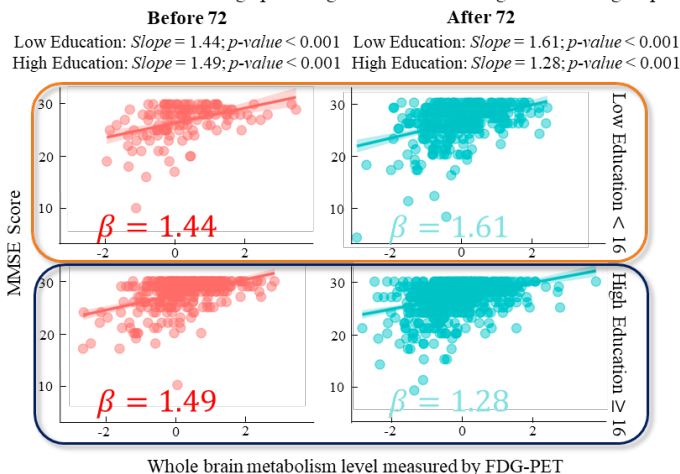


Fig. 11. (a) The T-MMSE relationship before (in red) and after (in green) the change point of age 78 for low-education (top) and high-education (bottom) groups. (b) The mediation analysis result of *APOE*→T→MMSE pathway before and after the change point for low-education (top) and high-education (bottom) groups.

a. Regression plot for MMSE score and whole brain metabolism level before and after the detected change points age 72 for low and high-education groups.



b. Graphical demonstration of mediation effect of metabolism level in *APOE4*→FDG→MMSE score stratified by low and high-education level.

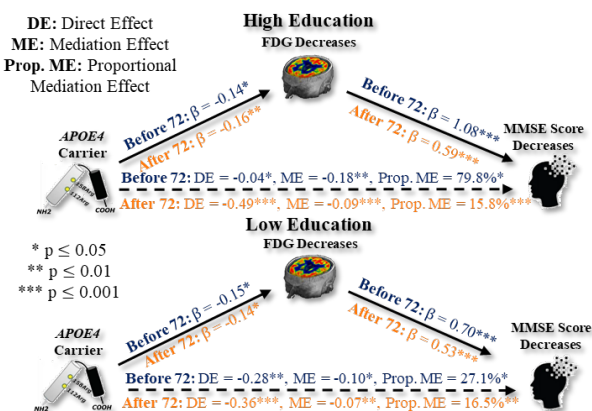
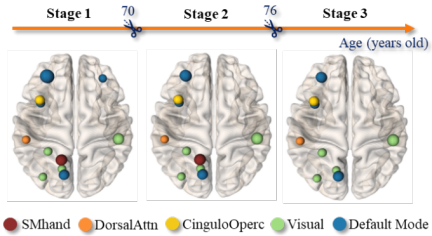


Fig. 12. (a) The [N]~MMSE relationship before (in red) and after (in green) the change point of age 72 for low-education (top) and high-education (bottom) groups. (b) The mediation analysis result of *APOE4*→[N]→MMSE pathway before and after the change point for low-education (top) and high-education (bottom) groups.

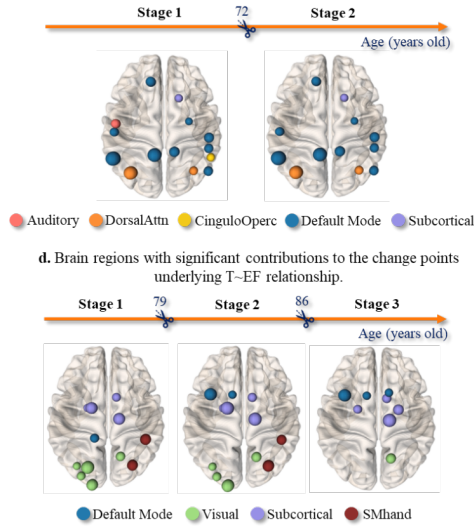
a. Estimated change points and p-values (sort by age) for EF. The results with significant p-value are bold.

| | 1st CP (p-value) | 2nd CP (p-value) |
|---------------|-----------------------|-----------------------|
| A Biomarker | 70 (<0.001) | 76 (<0.001) |
| T Biomarker | 79 (<0.001) | 86 (0.10) |
| [N] Biomarker | 72 (<0.001) | |

b. Brain regions with significant contributions to the change points underlying A~EF relationship.



c. Brain regions with significant contributions to the change points underlying [N]~EF relationship.



d. Brain regions with significant contributions to the change points underlying T~EF relationship.

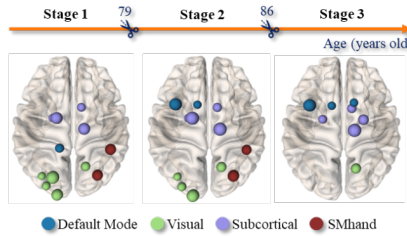


Fig. 13. Identified change points (sorted in age) and the associated *p*-value in the AT[N]~EF relationship are shown in (a). The brain regions showing significant contribution to the change points underlying A~EF, T~EF, and [N]~EF relationship are displayed in (b), (c), and (d), respectively. The node size and color indicate the effect size and topological location in the large-scale functional networks.

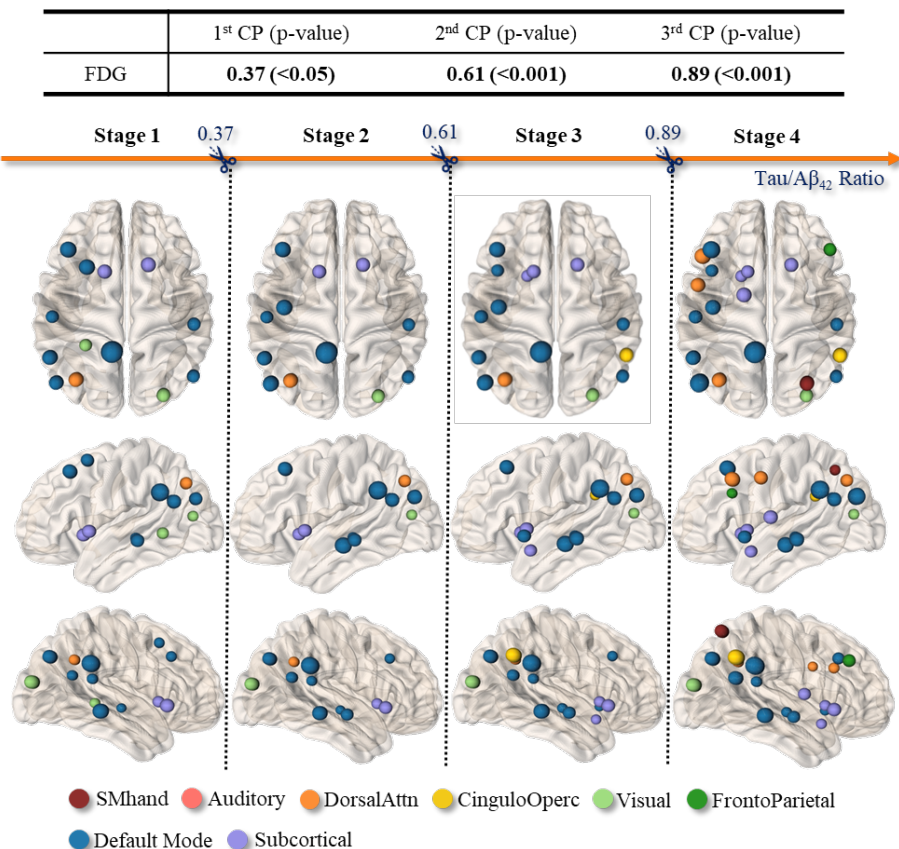


Fig. 14. Top: Three change points have been detected (sort by CSF $\text{tau}/\text{A}\beta_{42}$ biomarker) in $[N]$ -MMSE relationship. Bottom: The brain regions with strong contributions to the changes of $[N]$ -MMSE relationships prior to and after each change point.

(删除了: Tau/Aβ)

| | | Amyloid (N=1071) | Tau (N=245) | FDG (N=1360) |
|-------------------------------|-------------------|-------------------------|---------------------|---------------------|
| Age | Mean (SD) | 75.2 (7.64) | 78.3 (6.99) | 74.5 (7.41) |
| | Median [Min, Max] | 75.4 [55.2, 96.6] | 78.4 [61.4, 94.5] | 74.7 [55.2, 95.8] |
| Biological Sex | Male | 578 (54.0%) | 138 (56.3%) | 752 (55.3%) |
| | Female | 493 (46.0%) | 107 (43.7%) | 608 (44.7%) |
| Memory Composite Score | Mean (SD) | 0.331 (1.018) | 0.522 (0.888) | 0.274 (0.962) |
| | Median [Min, Max] | 0.423 [-2.86, 3.14] | 0.580 [-2.39, 2.72] | 0.331 [-2.86, 3.20] |
| EF Composite Score | Mean (SD) | 0.258 (1.127) | 0.566 (1.057) | 0.187 (1.098) |
| | Median [Min, Max] | 0.309 [-3.31, 2.99] | 0.565 [-2.72, 2.99] | 0.238 [-3.06, 2.99] |
| Education (Years) | Mean (SD) | 16.222 (2.671) | 16.523 (2.651) | 16.026 (2.764) |
| | Median [Min, Max] | 16 [6, 20] | 16 [6, 20] | 16 [6, 20] |
| APOE4 Status | Non-Carrier | 600 (56.0%) | 152 (62.0%) | 740 (54.4%) |
| | Carrier | 471 (44.0%) | 93 (38.0%) | 620 (45.6%) |
| AD Stage | CN-SMC | 376 (35.1%) | 126 (51.4%) | 439 (32.3%) |
| | EMCI | 298 (27.8%) | 68 (27.8%) | 301 (22.1%) |
| | LMCI-AD | 397 (37.1%) | 51 (20.8%) | 620 (45.6%) |

Table 1. Demographic characteristics of participants in amyloid, tau, and FDG change point detection.

| | Sample Size N and Dimension of Covariates P | % of Detecting Significant Change Point in 50 Replications | Average p-values for the First Detected Change Point in 50 Replications | Estimated Change Point Location: Mean with Standard Error |
|---------------------------------|---|--|---|---|
| No Change Point Case | N=500, P=100 | 6% | 0.42 | N/A |
| | N=500, P=200 | 8% | 0.53 | N/A |
| | N=1000, P=100 | 0% | 0.57 | N/A |
| | N=1000, P=200 | 2% | 0.58 | N/A |
| Single Change Point Case | N=500, P=100 | 100% | 0.00 | 74.96 (0.32) |
| | N=500, P=200 | 100% | 0.00 | 74.88 (0.31) |
| | N=1000, P=100 | 100% | 0.00 | 74.94 (0.19) |
| | N=1000, P=200 | 100% | 0.00 | 74.98 (0.18) |

Table 2. Simulation results for no change point case and single change point case.

| | 1 st Change Point (p-value) | 2 nd Change Point (p-value) | 3 rd Change Point (p-value) |
|---------------|--|--|--|
| A-Biomarker | Age 77 (0.40) | | |
| T-Biomarker | | Age 78 (0.001) | Age 72 (0.01) |
| [N]-Biomarker | | Age 72 (0.03) | Age 83 (0.025) |

Table 3. Estimated change points and p-values (sorted by age) using AD biomarkers. The change point detection results with p-value<0.1 are highlighted.

| | 1 st Change Point (p-value) | 2 nd Change Point (p-value) |
|---------------|--|--|
| A-Biomarker | 74 (0.47) | |
| T-Biomarker | 80 (0.07) | 86 (0.10) |
| [N]-Biomarker | 74 (0.93) | |

Table 4. Identified change points (sorted in age) and the associated p-value in the AT[N]~MEM relationship.